

**Fig. 4.** Unmodified mSP1000-induced IL-1 $\beta$  production is mediated by activation of NALP3 inflammasome. PMA-primed THP-1 cells transiently transfected with CFP-ASC were treated with unmodified mSP1000. The cells were then observed by confocal microscopy. Treated with unmodified mSP1000 alone (top); untreated but transfected with CFP-ASC (middle); or treated with unmodified mSP1000 and transfected with CFP-ASC (bottom). Arrows indicate clusters of CFP-ASC (blue).

#### 4. Discussion

Our goal was to elucidate the mechanisms of the inflammatory effects induced by SPs and to provide basic information for the creation of safe and effective SPs. To achieve these purposes, we focused on the IL-1 $\beta$  production induced by SPs, because IL-1 $\beta$  production is currently considered to play an important role in the initial inflammatory responses that lead to asbestosis and silicosis [19]. Our results provided evidence that unmodified mSP1000, but not smaller SPs, induces significant IL-1 $\beta$  production by THP-1 cells. Although the detailed mechanisms of this particle-size dependency in IL-1 $\beta$  production were unclear, we speculate that there are differences in the intracellular behavior of SPs and in the signaling pathways, and cytokine production patterns induced by SPs. Consistent with our hypothesis, our unpublished data showed that mSP1000s and the smaller SPs induce different inflammatory cytokine and chemokine production profiles (data not shown). Furthermore, many reports have shown that nanosized SPs induce inflammation *in vivo*. Therefore, we consider that it is also necessary to investigate the cytokine and chemokine production profiles induced by SPs of various sizes.

We then examined the effects of surface modification on mSP1000-induced IL-1 $\beta$  production, because it has become evident that surface properties are important factors in the biological effects of particles [14,15]. Interestingly, although unmodified and surface-modified mSP1000s were taken up equally, surface-

modified mSP1000s induce little or no IL-1 $\beta$  production (Fig. 1B). The *in vivo* inflammatory effect was similarly reduced by surface modification of mSP1000s (Fig. 1C). We consider these results important to the creation of safe SPs.

Next, we examined the mechanisms of IL-1 $\beta$  production induced by mSP1000s to elucidate why surface modification reduced IL-1 $\beta$  production. First, we revealed that mSP1000-induced IL-1 $\beta$  production depends on the activation of NLRP3 inflammasome by using CFP-ASC fusion protein (Fig. 4). Some reports showed that other inflammasomes such as NLRP1 could activate caspase-1 in an ASC-dependent way [35]. Therefore we will need to confirm a specific role for NLRP3 in IL-1 $\beta$  production induced by mSP1000s by using siRNA of NLRP3 in future. A recent study showed that NLRP3 inflammasome mediated IL-1 $\beta$  production is associated with fever syndromes characterized by spontaneous inflammation [21]. In fact, the IL-1 $\beta$  receptor antagonist anakinra has been successfully used to treat patients suffering from inflammatory diseases, indicating that these patients have underlying increased IL-1 $\beta$  production [36,37]. However, the mechanisms of NLRP3 activation remain unclear, and therefore the definitive target to be overcome for the creation of safe materials is still unknown. Recently, different groups separately reported that cathepsin B leakage after endosomal rupture, as well as cytoplasmic ROS, plays a crucial role in the activation of NLRP3 inflammasome [13,20]. Consistent with these notions, we demonstrated here that mSP1000-induced IL-1 $\beta$  production is mediated by cathepsin B and

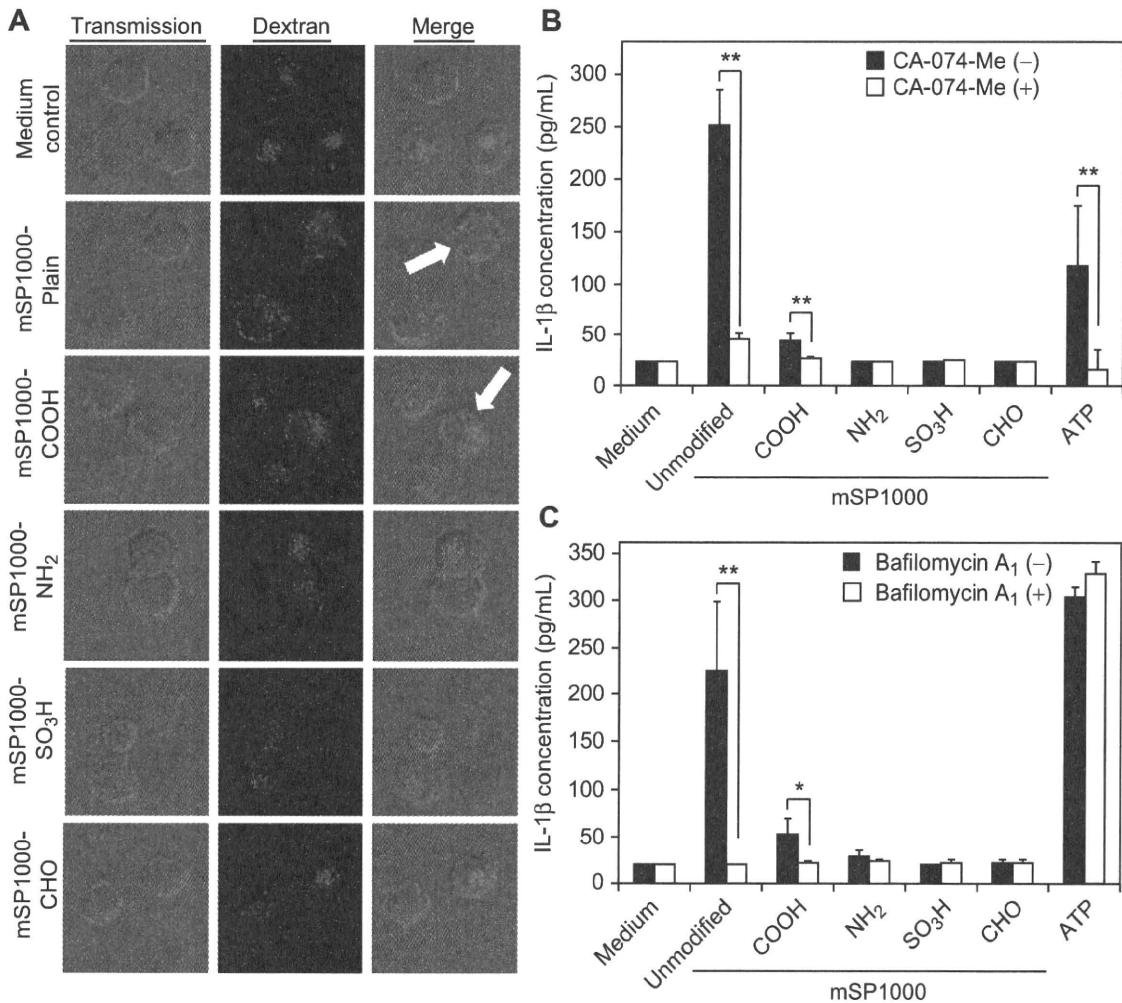


**Fig. 5.** mSP1000-induced IL-1 $\beta$  production is mediated by endosomal rupture. (A) Confocal microscopy of endosomal morphology. PMA-primed THP-1 cells were incubated with Alexa Fluor 594-conjugated dextran (red) and each type of mSP1000 for 6 h. The cells were then observed by confocal microscopy. Arrows show cells with spread of dextran into the cytoplasm, indicating endosomal rupture. (B, C) Involvement of cathepsin B in mSP1000-induced IL-1 $\beta$  production. PMA-primed THP-1 cells were treated with each type of mSP1000 or with ATP for 6 h in the absence (black bars) or presence (white bars) of (B) CA-074-Me (2  $\mu$ M) or (C) bafilomycin A<sub>1</sub> (250 nM). Data represent means  $\pm$  SD ( $n = 5$ ; \* $P < 0.05$ , \*\* $P < 0.01$  versus value for inhibitor [-] control within each treatment pair,  $t$ -test).

ROS (Figs. 5 and 6). However, it was unclear whether ROS and cathepsin B activate NLRP3 inflammasome separately or in a coordinated manner, and it was also unclear how endosomal rupture occurred. Use of a ROS inhibitor and surface-modified mSP1000s efficiently suppressed endosomal rupture (Fig. 6D). From these observations, we speculate that, with mSP1000 treatment, ROS trigger endosomal rupture and subsequent cathepsin B leakage into the cytosol, leading to the activation of NLRP3 inflammasome (Fig. 7). Our hypothesis is consistent with some reports suggesting that ROS trigger destabilization of the lysosomal membrane by membrane lipid oxidation [38].

In contrast, some reports have suggested that, in the case of crystalline silica, the reactive particle surface interacts with phagolysosomal membranes, leading to the release of endosomal enzymes into the cytosol after phagocytosis [39–41]. These contradictory findings suggest that various materials induce biological effects by different mechanisms in response to differences in particle characteristics. However, it remains unclear why the surface modification of mSP1000 reduced ROS production. It is possible that inappropriate surface modification induces an

inflammatory effect stronger than that of unmodified SP. We consider that further studies of the relationship between surface characteristics and bio-effect are necessary for the development of safe and effective materials. In this report, we found that DPI, an inhibitor of NADPH oxidase, significantly suppressed mSP1000-induced IL-1 $\beta$  production (Fig. 6C). NADPH oxidase is activated by the assembly of membrane lipids at local sites on the cellular surface and in the cytoplasm where the particles attach [42,43]. At this point, the silanol group (Si-OH) induces binding of the particles to membranes [44,45]. Therefore, we speculate that surface modification of mSP1000 masks the silanol group from the surface of the mSP1000 and blocks subsequent NADPH oxidase activation.

On the other hand, SP-induced cell death is also a critical obstacle, because macrophages play a central role in host defense systems. In 2007, Willingham et al. proposed a novel cell death pathway called pyronecrosis [46]. Induction of pyronecrosis is not dependent on IL-1 $\beta$  signaling or caspase-1 activity, although it requires the presence of the inflammasome component ASC and cathepsin B [46–48]. Our data suggested that mSP1000-induced cell death is independent of caspase-1 and IL-1 $\beta$  signaling but

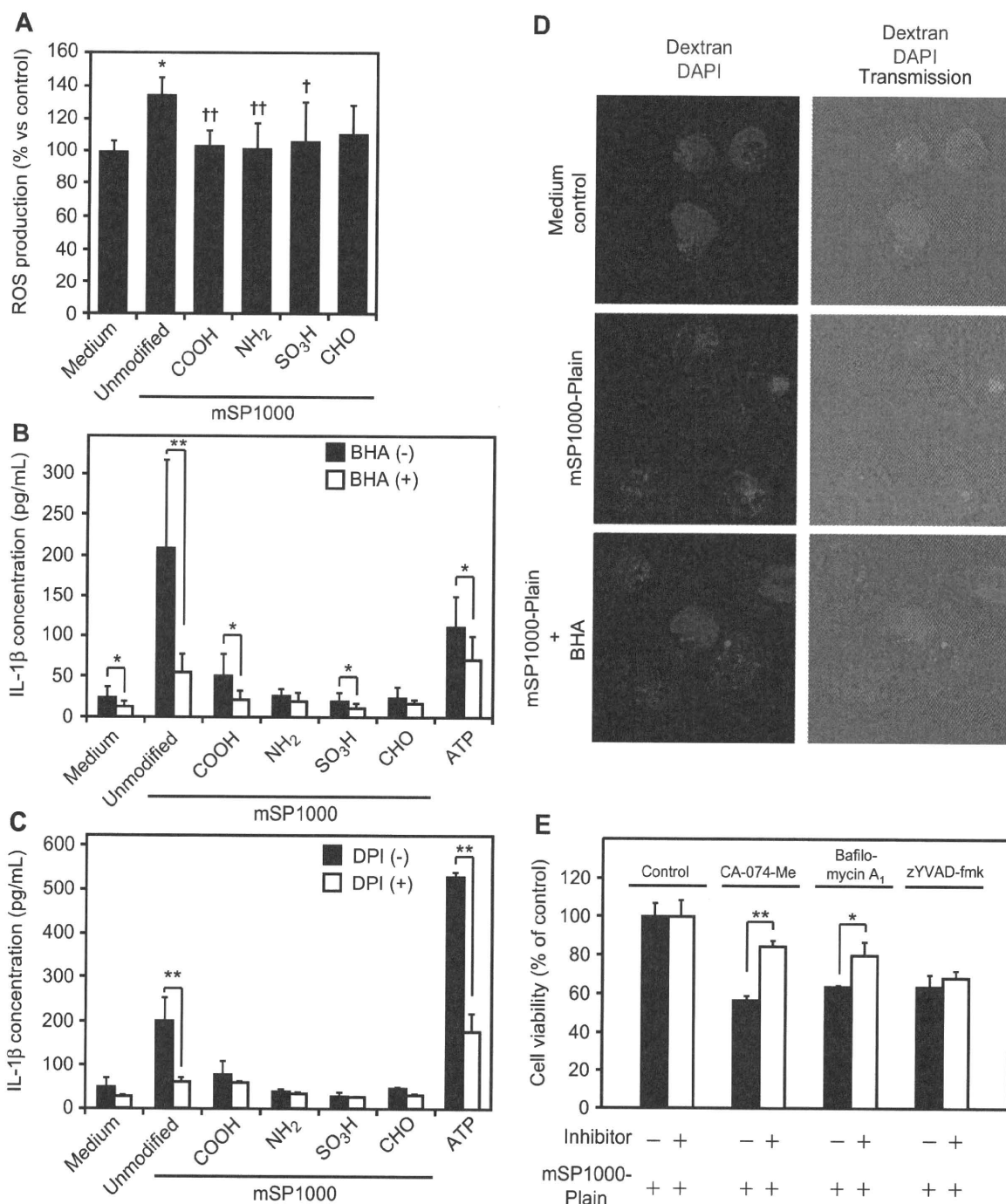


**Fig. 6.** Unmodified mSP1000-induced ROS production induces endosomal rupture and subsequent IL-1 $\beta$  production. (A) ROS production levels in PMA-primed THP-1 cells. Cells were treated with each type of mSP1000 for 24 h and incubated with H<sub>2</sub>DCFDA (10  $\mu$ M) for 45 min. Fluorescence was then measured at OD<sub>485–530</sub>. ROS production intensity was calculated by the formula ROS production intensity = fluorescence/number of live cells. ROS production intensity of untreated control cells was arbitrarily set to 100%. Data represent means  $\pm$  SD ( $n = 5$ ; \* $P < 0.05$  versus value for PBS control, <sup>†</sup> $P < 0.05$ , <sup>††</sup> $P < 0.01$  versus value for unmodified mSP1000, ANOVA). (B, C) Involvement of ROS in mSP1000-induced IL-1 $\beta$  production. PMA-primed THP-1 cells were treated with each type of mSP1000 or with ATP for 6 h in the absence (black bars) or presence (white bars) of (B) BHA (150  $\mu$ M) or (C) DPI (60  $\mu$ M), and IL-1 $\beta$  production levels were measured by ELISA. (D) Confocal microscopy of endosomal morphology. PMA-primed THP-1 cells were incubated with Alexa Fluor 594-conjugated dextran (red) and unmodified mSP1000 for 6 h in the presence (bottom) or absence (middle) of BHA (150  $\mu$ M). Cells were then observed by confocal microscopy. Arrows indicate cells with spread of dextran into the cytoplasm. (E) Involvement of cathepsin B and caspase-1 in unmodified mSP1000-induced cytotoxicity. PMA-primed THP-1 cells were treated with unmodified mSP1000 for 24 h in the absence (black bars) or presence (white bars) of CA-074-Me (2  $\mu$ M), bafilomycin A<sub>1</sub> (250 nM), or zYVAD-fmk (10  $\mu$ M). Cell viability was measured by methylene blue assay. Data represent means  $\pm$  SD ( $n = 5$ ; \* $P < 0.05$ , \*\* $P < 0.01$  versus value for inhibitor [–] control within each treatment pair,  $t$ -test).

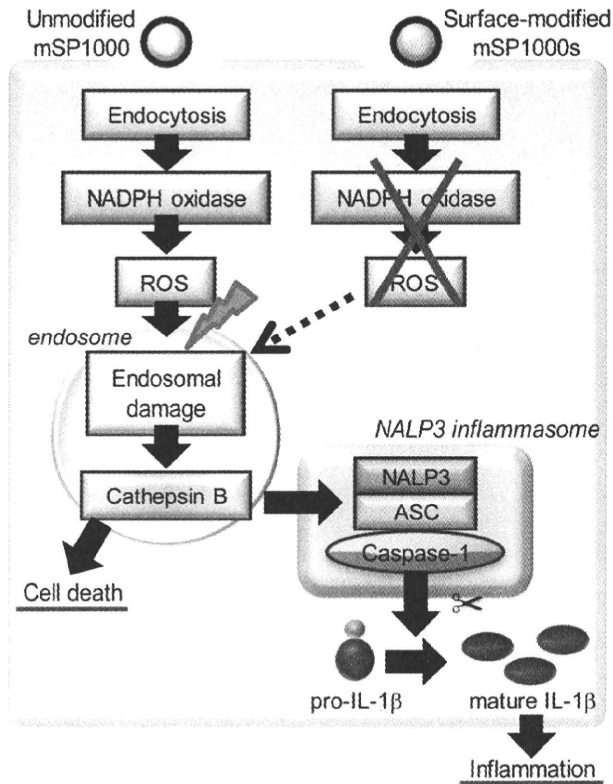


**Fig. 7.** Model of mSP1000-induced IL-1 $\beta$  maturation pathways. Unmodified mSP1000-induced IL-1 $\beta$  maturation is mediated by phagocytosis, activation of NADPH oxidase, ROS production, endosomal rupture, active cathepsin B leakage, assembly of NALP3 inflammasome, and caspase-1 activation. Surface-modified mSP1000s do not activate NADPH oxidase or ROS production, although they are taken up at the same rate as unmodified mSP1000.

dependent on cathepsin B (Fig. 6E) with the ASC assembly (Fig. 4), which means that unmodified mSP1000-induced cell death might occur by pyronecrosis. Pyronecrosis is considered to elicit substantial inflammation and to affect the local environment, whereas apoptosis is widely accepted as non-inflammatory cell death without effects around the dying cells [48]. Thus, pyronecrosis is likely to contribute substantially to the disease state in patients with inflammatory diseases.

We revealed here that SP-induced ROS act as an important upstream signal in the NLRP3 activation pathway. Moreover, we showed that modification of mSP1000s with functional groups suppressed their inflammatory effects. We have since obtained similar results with nanosized particles (nSP70) (unpublished data). These results support our hypothesis that appropriate surface modification of SPs suppresses their inflammatory effect. However, we speculate that blind modification could exacerbate the inflammatory effect, and we consider that an analysis of the mechanisms of the phenomena reported here is necessary.

## 5. Conclusions

We reveal here that unmodified mSP1000-induced IL-1 $\beta$  production is mediated by the activation of NADPH oxidase, ROS production, endosomal rupture, active cathepsin B leakage, assembly of NLRP3 inflammasome, and caspase-1 activation. Furthermore, by surface modification with functional groups, we successfully suppressed unmodified mSP1000-induced ROS

production, an upstream signal in the NLRP3 activation pathway, and the subsequent inflammatory responses or cell death. We consider that further studies of the relationship between surface characteristics and biological effects would lead to the development of safe and effective SPs.

## Acknowledgements

The authors declare that they have no conflict of interests. We thank Dr. D.T. Golenbock (Department of Infectious Diseases and Immunology, University of Massachusetts Medical School) for providing CFP-ASC plasmid. This study was supported in part by grants from the Ministry of Health, Labor, and Welfare of Japan; by the Ministry of the Environment of Japan; and by the Global COE Program "In Silico Medicine" at Osaka University.

## Appendix

Figures with essential color discrimination. Figs. 2, 4–7 in this article are difficult to interpret in black and white. The full color images can be found in the on-line version, at doi:10.1016/j.biomaterials.2010.05.036.

## References

- [1] Mossman BT, Churg A. Mechanisms in the pathogenesis of asbestosis and silicosis. *Am J Respir Crit Care Med* 1998;157:1666–80.
- [2] Huaux F. New developments in the understanding of immunology in silicosis. *Curr Opin Allergy Clin Immunol* 2007;7:168–73.
- [3] Hirsch LR, Stafford RJ, Bankson JA, Sershen SR, Rivera B, Price RE, et al. Nanoshell-mediated near-infrared thermal therapy of tumors under magnetic resonance guidance. *Proc Natl Acad Sci U S A* 2003;100:13549–54.
- [4] Bharali DJ, Klejbor I, Stachowiak EK, Dutta P, Roy I, Kaur N, et al. Organically modified silica nanoparticles: a nonviral vector for in vivo gene delivery and expression in the brain. *Proc Natl Acad Sci U S A* 2005;102:11539–44.
- [5] Roy I, Ohulchanskyy TY, Bharali DJ, Pudavar HE, Mistretta RA, Kaur N, et al. Optical tracking of organically modified silica nanoparticles as DNA carriers: a nonviral, nanomedicine approach for gene delivery. *Proc Natl Acad Sci U S A* 2005;102:279–84.
- [6] Bottini M, D'Annibale F, Magrini A, Cerignoli F, Arimura Y, Dawson MI, et al. Quantum dot-doped silica nanoparticles as probes for targeting of T-lymphocytes. *Int J Nanomedicine* 2007;2:227–33.
- [7] Verraedt E, Pendela M, Adams E, Hoogmartens J, Martens JA. Controlled release of chlorhexidine from amorphous microporous silica. *J Contr Release* 2010;142:47–52.
- [8] Wiethoff AJ, Reed KL, Webb TR, Warheit DB. Assessing the role of neutrophil apoptosis in the resolution of particle-induced pulmonary inflammation. *Inhal Toxicol* 2003;15:1231–46.
- [9] Cho WS, Choi M, Han BS, Cho M, Oh J, Park K, et al. Inflammatory mediators induced by intratracheal instillation of ultrafine amorphous silica particles. *Toxicol Lett* 2007;175:24–33.
- [10] Park EJ, Park K. Oxidative stress and pro-inflammatory responses induced by silica nanoparticles in vivo and in vitro. *Toxicol Lett* 2009;184:18–25.
- [11] Akerman ME, Chan WC, Laakkonen P, Bhatia SN, Ruoslahti E. Nanocrystal targeting in vivo. *Proc Natl Acad Sci U S A* 2002;99:12617–21.
- [12] Kirchner C, Liedl T, Kudera S, Pellegrino T, Munoz Javier A, Gaub HE, et al. Cytotoxicity of colloidal CdSe and CdSe/ZnS nanoparticles. *Nano Lett* 2005;5:331–8.
- [13] Dostert C, Petrilli V, Van Bruggen R, Steele C, Mossman BT, Tschopp J. Innate immune activation through Nalp3 inflammasome sensing of asbestos and silica. *Science* 2008;320:674–7.
- [14] Albrecht C, Schins RP, Hohr D, Becker A, Shi T, Knaapen AM, et al. Inflammatory time course after quartz instillation: role of tumor necrosis factor- $\alpha$  and particle surface. *Am J Respir Cell Mol Biol* 2004;31:292–301.
- [15] He X, Nie H, Wang K, Tan W, Wu X, Zhang P. In vivo study of biodistribution and urinary excretion of surface-modified silica nanoparticles. *Anal Chem* 2008;80:9597–603.
- [16] Waters KM, Masiello LM, Zangar RC, Tarasevich BJ, Karin NJ, Quesenberry RD, et al. Macrophage responses to silica nanoparticles are highly conserved across particle sizes. *Toxicol Sci* 2009;107:553–69.
- [17] Dinarello CA. Interleukin-1 beta, interleukin-18, and the interleukin-1 beta converting enzyme. *Ann N Y Acad Sci* 1998;856:1–11.
- [18] Petrilli V, Dostert C, Muruve DA, Tschopp J. The inflammasome: a danger sensing complex triggering innate immunity. *Curr Opin Immunol* 2007;19:615–22.



- [19] Cassel SL, Eisenbarth SC, Iyer SS, Sadler JJ, Colegio OR, Tephly LA, et al. The Nalp3 inflammasome is essential for the development of silicosis. *Proc Natl Acad Sci U S A* 2008;105:9035–40.
- [20] Hornung V, Bauernfeind F, Halle A, Samstad EO, Kono H, Rock KL, et al. Silica crystals and aluminum salts activate the NALP3 inflammasome through phagosomal destabilization. *Nat Immunol* 2008;9:847–56.
- [21] Ting JP, Kastner DL, Hoffman HM. CATERPILLERS, pyrin and hereditary immunological disorders. *Nat Rev Immunol* 2006;6:183–95.
- [22] Martinon F, Petrilli V, Mayor A, Tardivel A, Tschopp J. Gout-associated uric acid crystals activate the NALP3 inflammasome. *Nature* 2006;440:237–41.
- [23] Agostini L, Martinon F, Burns K, McDermott MF, Hawkins PN, Tschopp J. NALP3 forms an IL-1 $\beta$ -processing inflammasome with increased activity in Muckle-Wells autoinflammatory disorder. *Immunity* 2004;20:319–25.
- [24] Mariathasan S, Weiss DS, Newton K, McBride J, O'Rourke K, Roose-Girma M, et al. Cryopyrin activates the inflammasome in response to toxins and ATP. *Nature* 2006;440:228–32.
- [25] Halle A, Hornung V, Petzold GC, Stewart CR, Monks BG, Reinheckel T, et al. The NALP3 inflammasome is involved in the innate immune response to amyloid- $\beta$ . *Nat Immunol* 2008;9:857–65.
- [26] Shio MT, Eisenbarth SC, Savaria M, Vinet AF, Bellemare MJ, Harder KW, et al. Malarial hemozoin activates the NLRP3 inflammasome through Lyn and Syk kinases. *PLoS Pathog* 2009;5:e1000559.
- [27] Yoshioka Y, Watanabe H, Morishige T, Yao X, Ikemizu S, Nagao C, et al. Creation of lysine-deficient mutant lymphotoxin- $\alpha$  with receptor selectivity by using a phage display system. *Biomaterials* 2010;31:1935–43.
- [28] Busuttill SJ, Ploplis VA, Castellino FJ, Tang L, Eaton JW, Plow EF. A central role for plasminogen in the inflammatory response to biomaterials. *J Thromb Haemost* 2004;2:1798–805.
- [29] Chung EY, Kim SJ, Ma XJ. Regulation of cytokine production during phagocytosis of apoptotic cells. *Cell Res* 2006;16:154–61.
- [30] Fernandes-Alnemri T, Wu J, Yu JW, Datta P, Miller B, Jankowski W, et al. The pyroptosome: a supramolecular assembly of ASC dimers mediating inflammatory cell death via caspase-1 activation. *Cell Death Differ* 2007;14:1590–604.
- [31] Magalhaes AC, Baron GS, Lee KS, Steele-Mortimer O, Dorward D, Prado MA, et al. Uptake and neuritic transport of scrapie prion protein coincident with infection of neuronal cells. *J Neurosci* 2005;25:5207–16.
- [32] Egler RA, Fernandes E, Rothermund K, Sereika S, de Souza-Pinto N, Jaruga P, et al. Regulation of reactive oxygen species, DNA damage, and c-Myc function by peroxiredoxin 1. *Oncogene* 2005;24:8038–50.
- [33] Morel F, Doussiere J, Vignais PV. The superoxide-generating oxidase of phagocytic cells. Physiological, molecular and pathological aspects. *Eur J Biochem* 1991;201:523–46.
- [34] Morishige A, Yoshioka Y, Inakura H, Tanabe A, Yao X, Tsunoda SI, et al. Cytotoxicity of amorphous silica particles against macrophage-like THP-1 cells depends on particle-size and surface properties. *Pharmazie* in press.
- [35] Franchi L, Eigenbrod T, Munoz-Planillo R, Nunez G. The inflammasome: a caspase-1-activation platform that regulates immune responses and disease pathogenesis. *Nat Immunol* 2009;10:241–7.
- [36] Piguet PF, Vesin C, Grau GE, Thompson RC. Interleukin 1 receptor antagonist (IL-1ra) prevents or cures pulmonary fibrosis elicited in mice by bleomycin or silica. *Cytokine* 1993;5:57–61.
- [37] Hawkins PN, Lachmann HJ, McDermott MF. Interleukin-1-receptor antagonist in the Muckle-Wells syndrome. *N Engl J Med* 2003;348:2583–4.
- [38] Kurz T, Terman A, Gustafsson B, Brunk UT. Lysosomes and oxidative stress in aging and apoptosis. *Biochim Biophys Acta* 2008;1780:1291–303.
- [39] Allison AC, Harington JS, Birbeck M. An examination of the cytotoxic effects of silica on macrophages. *J Exp Med* 1966;124:141–54.
- [40] Nadler S, Goldfischer S. The intracellular release of lysosomal contents in macrophages that have ingested silica. *J Histochem Cytochem* 1970;18:368–71.
- [41] Erdogdu G, Hasirci V. An overview of the role of mineral solubility in silicosis and asbestosis. *Environ Res* 1998;78:38–42.
- [42] Ng G, Sharma K, Ward SM, Desrosiers MD, Stephens LA, Schoel WM, et al. Receptor-independent, direct membrane binding leads to cell-surface lipid sorting and Syk kinase activation in dendritic cells. *Immunity* 2008;29:807–18.
- [43] Kuijk LM, Beekman JM, Koster J, Waterham HR, Frenkel J, Coffey PJ. HMG-CoA reductase inhibition induces IL-1 $\beta$  release through Rac1/PI3K/PKB-dependent caspase-1 activation. *Blood* 2008;112:3563–73.
- [44] Nash T, Allison AC, Harington JS. Physico-chemical properties of silica in relation to its toxicity. *Nature* 1966;210:259–61.
- [45] Pandurangi RS, Seehra MS, Razzaboni BL, Bolsaitis P. Surface and bulk infrared modes of crystalline and amorphous silica particles: a study of the relation of surface structure to cytotoxicity of respirable silica. *Environ Health Perspect* 1990;86:327–36.
- [46] Willingham SB, Bergstralh DT, O'Connor W, Morrison AC, Taxman DJ, Duncan JA, et al. Microbial pathogen-induced necrotic cell death mediated by the inflammasome components CIAS1/cryopyrin/NLRP3 and ASC. *Cell Host Microbe* 2007;2:147–59.
- [47] Fujisawa A, Kambe N, Saito M, Nishikomori R, Tanizaki H, Kanazawa N, et al. Disease-associated mutations in CIAS1 induce cathepsin B-dependent rapid cell death of human THP-1 monocytic cells. *Blood* 2007;109:2903–11.
- [48] Ting JP, Willingham SB, Bergstralh DT. NLRs at the intersection of cell death and immunity. *Nat Rev Immunol* 2008;8:372–9.

Laboratory of Biotechnology and Therapeutics<sup>1</sup>, Graduate School of Pharmaceutical Sciences; The Center for Advanced Medical Engineering and Informatics<sup>2</sup>, Osaka University; Laboratory of Pharmaceutical Proteomics<sup>3</sup>, National Institute of Biomedical Innovation, Laboratory of Toxicology and Safety Science<sup>4</sup>, Graduate School of Pharmaceutical Sciences, Osaka University, Osaka, Japan

## Cytotoxicity of amorphous silica particles against macrophage-like THP-1 cells depends on particle-size and surface properties

T. MORISHIGE<sup>1,\*</sup>, Y. YOSHIOKA<sup>1,2,\*</sup>, H. INAKURA<sup>1</sup>, A. TANABE<sup>1</sup>, X. YAO<sup>1</sup>, S. TSUNODA<sup>2,3</sup>, Y. TSUTSUMI<sup>2,3,4</sup>, Y. MUKAI<sup>1</sup>, N. OKADA<sup>1</sup>, S. NAKAGAWA<sup>1,2</sup>

Received December 17, 2009, accepted January 4, 2010

Yasuo Yoshioka, Ph.D., The Center for Advanced Medical Engineering and Informatics, Osaka University, 1-6 Yamadaoka, Suita, Osaka 565-0871, Japan  
yasuo@phs.osaka-u.ac.jp

\* Each author contributed equally to the work.

Pharmazie 65: 1–4 (2010)

doi: 10.1691/ph.2010.9408

Recent studies have indicated that amorphous silica particles (SPs) show cytotoxicity against various types of cells, including macrophages. However, the mechanism of cell death has not been determined, and systematic investigations of the relationship between particle characteristics and cytotoxicity are still quite limited. Here, we compared the cytotoxicity of SPs of various sizes (30–1000 nm) and surface properties against differentiated THP-1 human macrophage-like cells. We found that 300 and 1000 nm SPs showed cytotoxicity against THP-1 cells, whereas 30, 50, and 70 nm SPs did not induce cell death. We demonstrated that 1000 nm SP showed strong cytotoxicity that depended on reactive oxygen species but was independent of caspases. Furthermore, we showed that surface modification of 1000 nm SPs dramatically suppressed their cytotoxicity. Our results suggest that systematic evaluation of the association between particle characteristics and biological effects is necessary for the creation of safe SPs.

### 1. Introduction

Amorphous (noncrystalline) silica particles (SPs) possess useful properties, including straightforward synthesis, relatively low cost, easy separation, high hydrophilicity, and facile surface modification. In addition, SPs are usually considered to have low toxicity, in contrast to crystalline silica, which can cause silicosis and some forms of lung cancer (Mossman and Churg 1998; Huaux 2007). Therefore, SPs have been used for many applications, including cosmetics, foods, medical diagnosis, cancer therapy, and drug delivery (Hirsch et al. 2003; Bharali et al. 2005; Roy et al. 2005; Bottini et al. 2007; Verraedt et al. 2009).

However, the increasing use of SPs has raised public concern about their safety. In fact, recent studies have found that SPs induce substantial lung inflammation and are cytotoxic against various cells, including macrophages (Wiethoff et al. 2003; Cho et al. 2007; Napierska et al. 2009). Thus, the safety and overall biological effects of SPs have been questioned (Akerman et al. 2002; Kirchner et al. 2005; Dostert et al. 2008). In addition, it has recently become evident that particle characteristics, including particle size and surface properties, are important factors in pathologic alterations and cellular responses (Albrecht et al. 2004; He et al. 2008; Waters et al. 2009). Therefore, investigation of the mechanisms of SP-induced inflammation and cytotoxicity and of the relationship between particle characteristics and cytotoxicity is important for the development of safe SPs.

Here we demonstrate that SPs exhibit cytotoxicity against THP-1 human macrophage-like cells in a size-dependent man-

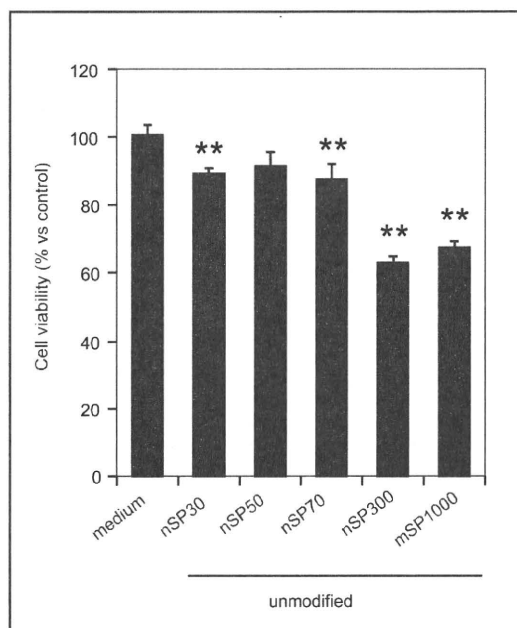


Fig. 1: Correlation between SP particle size and cytotoxicity against macrophage-like cells. PMA-primed THP-1 cells were treated with 100  $\mu$ g/mL unmodified SPs for 24 h, and cell viability was evaluated by means of the standard methylene blue assay. The data represent the mean  $\pm$  SD ( $n=5$ ; \*\* $P<0.01$  versus value for medium control)

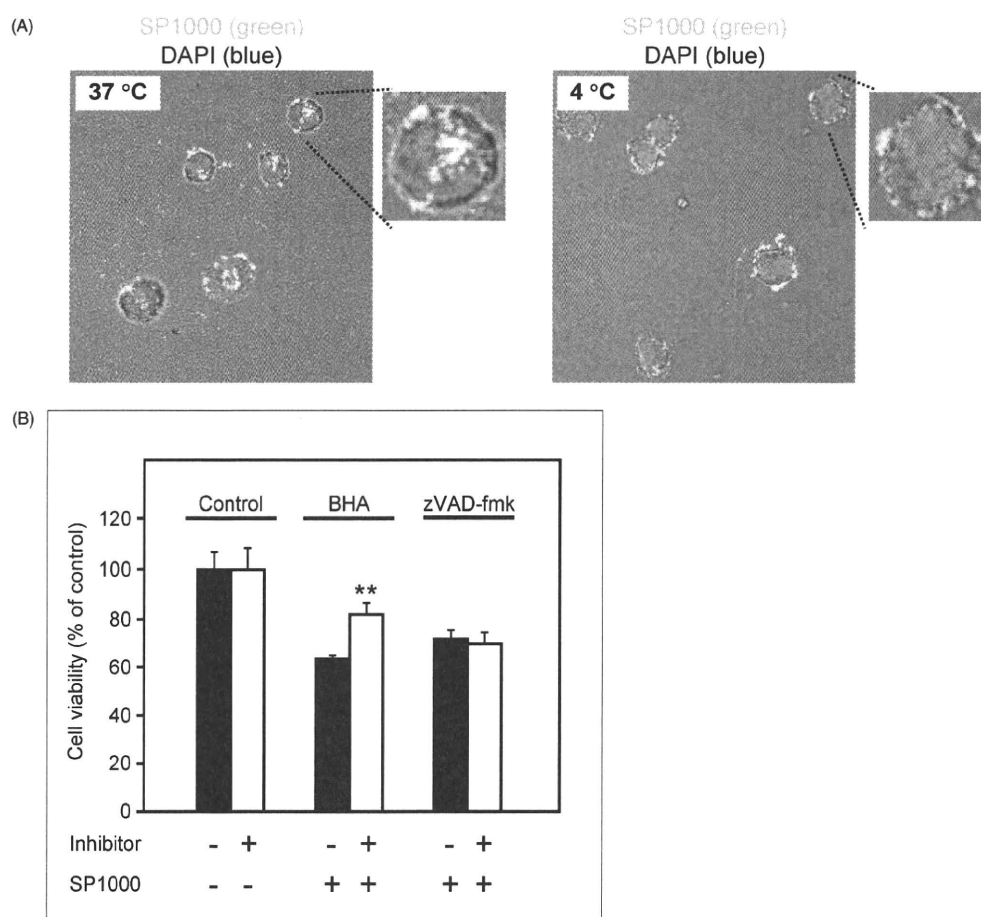


Fig. 2: ROS and caspase dependence of mSP1000-induced cell death. (A) Confocal microscopy images of the ingestion of mSP1000. FITC-conjugated mSP1000 (green) were added to the PMA-primed THP-1 cells at 100  $\mu\text{g}/\text{mL}$ . Cells were incubated for 6 h at 37 °C (left) or 4 °C (right). The nucleus was stained with DAPI (blue). (B) Effect of a caspase inhibitor and an ROS scavenger on cytotoxicity of mSP1000. PMA-primed THP-1 cells were treated with 100 (g/mL SP1000s for 24 h in the presence or absence of BHA (150  $\mu\text{M}$ ) or zVAD-fmk (60  $\mu\text{M}$ ). Cell viability was measured by means of the methylene blue assay. The data represent the mean  $\pm$  SD ( $n=4$ ; \*\* $P < 0.01$  versus value for inhibitor [-] control)

ner. Furthermore, we show that SPs with diameters of 1000 nm induce the production of reactive oxygen species (ROS), which triggers THP-1 cell death. We also demonstrate that surface modification of SPs with various functional groups significantly suppresses SP cytotoxicity.

## 2. Investigations, results and discussion

In this study, we examined whether the size and surface characteristics of SPs are correlated with their cytotoxicity. We also investigated the mechanism by which SPs induce the death of macrophage-like THP-1 cells, with the goal of providing information for the creation of novel safe SPs.

### 2.1. Amorphous silica particles induce cell death in a size-dependent manner

We used five SPs with diameters between 30 and 1000 nm (nSP30, nSP50, nSP70, nSP300, and mSP1000); the mean secondary particle diameters of the SPs measured by means of a Zetasizer were 33, 44, 79, 326, and 945 nm, respectively

(data not shown). To compare the cytotoxicities of the SPs with different diameters, we examined their cytotoxicity against macrophages, which are the first line of defense against infection or injury from various inhaled agents. We incubated phorbol 12-myristate 13-acetate (PMA)-primed human macrophage-like THP-1 cells with SPs and analyzed the levels of cell viability. Twenty-four hours after the incubation, we found that nSP300 and mSP1000 induced marked cytotoxicity, whereas nSP30, nSP50, and nSP70 showed no cytotoxicity (Fig. 1). These results indicate that the particle size of the SPs was intimately involved in their biological effects.

### 2.2. mSP1000-induced cytotoxicity depends on ROS but not on caspases

Macrophages remove inhaled agents including foreign particles by means of their phagocytic activity. To confirm that THP-1 cells took up mSP1000, we treated THP-1 cells with fluorescein-5-isothiocyanate (FITC)-conjugated mSP1000 at 37 °C or 4 °C. We visually confirmed that mSP1000 were ingested into THP-1 cells at 37 °C, whereas only adsorption of mSP1000 on the cellular surface was detected at 4 °C (Fig. 2A). These results

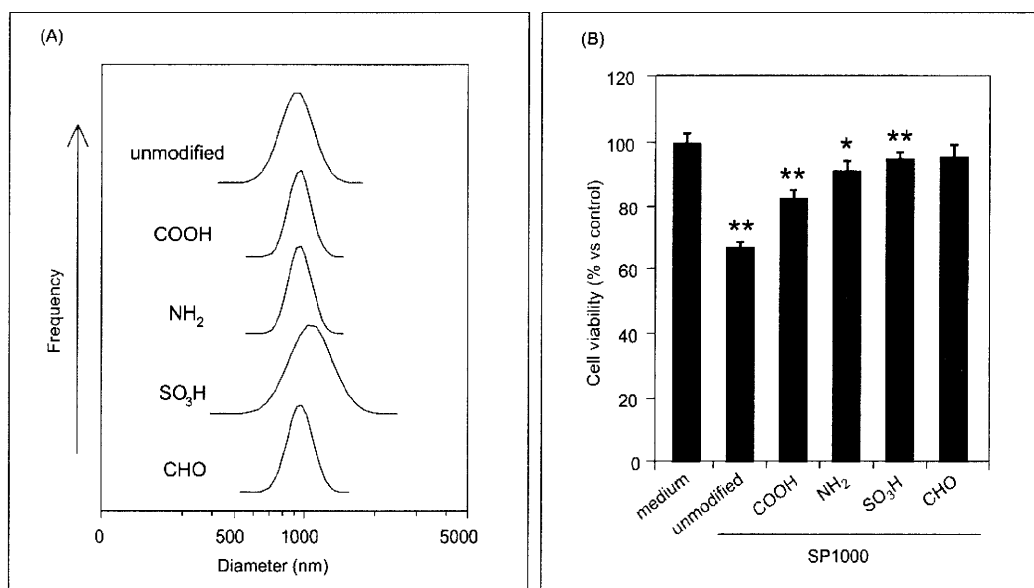


Fig. 3: Correlation between surface modification of mSP1000s and cytotoxicity against macrophage-like THP-1 cells. (A) Particle size distributions of unmodified and surface-modified mSP1000s. Particle size distributions were measured with a Zetasizer 3000HS after sonication at a particle concentration of 300 (g/mL in H<sub>2</sub>O). (B) Cytotoxicity of surface-modified mSP1000s. PMA-primed THP-1 cells were treated with the surface-modified mSP1000s at 100 µg/mL for 24 h. After the stimulation, cell viability was measured by means of the standard methylene blue assay. The data represent the mean ± SD ( $n=5$ ; \*\* $P<0.01$ , \* $P<0.05$  versus value for medium control)

indicate that mSP1000 were recognized and taken up into THP-1 cells by energy-dependent phagocytosis.

We next examined the mechanism of mSP1000-induced cytotoxicity. To determine whether there was an association between caspases and mSP1000-induced cell death, we treated cells with mSP1000 in the presence or absence of zVAD-fmk, a broad caspase inhibitor (it inhibits caspase-1, -3, -4, and -7). We found that zVAD-fmk did not affect the mSP1000-induced cytotoxicity, which indicates that the cytotoxicity was independent of caspases (Fig. 2B). Recently, four kinds of cell death pathways were reported: apoptosis, necrosis, pyroptosis, and pyronecrosis (Ting et al. 2008). Apoptosis and pyroptosis are dependent on the activity of caspases, whereas necrosis and pyronecrosis are independent of caspases. Therefore, our results suggest that mSP1000-induced cell death might have been necrosis or pyronecrosis. Both pathways elicit substantial inflammation, whereas apoptosis is a non-inflammatory cell death that does not affect the area around the dying cells (Ting et al. 2008). Therefore, we suspected that SP-induced cell death might be associated with inflammatory responses induced by mSP1000. However, the stimulation of macrophages with materials such as silica is known to induce ROS production (Msiska et al. 2009). Excessive production of ROS itself causes irreversible cellular injuries and contributes to the pathogenesis of several inflammatory diseases (Cross et al. 1994; Terman et al. 2006). To determine whether ROS were involved in mSP1000-induced cell death, we stimulated THP-1 cells with mSP1000 in the presence of a broad ROS scavenger, butylated hydroxyanisole (BHA), and found that the scavenger significantly inhibited the cytotoxicity of mSP1000 (Fig. 2B). These results indicate that ROS played an important role in the mSP1000-induced cell death and that the cytotoxicity induced by mSP1000 depends on ROS production but is independent of caspases, which suggests that mSP1000-induced cell death is inflammatory necrosis or pyronecrosis.

Pharmazie 65 (2010)

### 2.3. mSP1000-induced cell death is suppressed by surface modification with functional groups

To assess the correlation between surface modification and SP cytotoxicity, we used mSP1000 modified with various surface functional groups (-COOH, -NH<sub>2</sub>, -SO<sub>3</sub>H, and -CHO). The mean secondary particle diameters of unmodified mSP1000 was 945 nm, and the corresponding values for the modified particles were 1022, 958, 1023, and 969 nm, respectively (Fig. 3A). We compared the cytotoxicity of the modified and unmodified particles against THP-1 cells and found that mSP1000-induced cytotoxicity was suppressed by the surface modification (Fig. 3B). Interestingly, we confirmed that all the surface-modified mSP1000 were taken up equally into the cells (data not shown). We expect that surface modification can be used as a novel method to create safe SPs.

In summary, we confirmed that the cytotoxicity of SPs depended on particle size and surface properties. We confirmed that mSP1000-induced cell death was dependent on ROS production but independent of caspases. We believe that this information will be useful for the creation of novel safe SP-based materials.

## 3. Experimental

### 3.1. Materials and reagents

We used SPs with diameters between 30 and 1000 nm (nSP30, nSP50, nSP70, nSP300, and mSP1000), and mSP1000s with various surface functional groups (-COOH, -NH<sub>2</sub>, -SO<sub>3</sub>H, and -CHO). The SPs (Sicaster) were purchased from Micromod Partikeltechnologie (Rostock/Warnemünde, Germany). PMA and BHA were purchased from Sigma (St. Louis, MO). zVAD-fmk was purchased from Merck Calbiochem (Darmstadt, Germany).

### 3.2. Cell treatment

THP-1 cells (human acute monocytic leukemia cell line) were obtained from the American Type Culture Collection (Manassas, VA) and were cultured in RPMI-1640 (Wako Pure Chemical Industries, Osaka, Japan) supplemented

with 10% fetal bovine serum, 2 mM L-glutamine, and antibiotics at 37 °C. Treatment of THP-1 cells with PMA reportedly induces differentiation to a macrophage phenotype (Hoff et al. 1992; Rutault et al. 2001).

### 3.3. Size distribution of silica particles

The size distributions of the SP were measured with a Zetasizer 3000HS (Malvern, Worcestershire, UK) after sonication at a particle concentration of 300 µg/mL in H<sub>2</sub>O.

### 3.4. Cytotoxicity of various silica particles

THP-1 cells (1.5 × 10<sup>4</sup> cells/well) were seeded in 96-well plates, differentiated to macrophages by incubation with 0.5 (M PMA for 24 h, and then washed once with incubation medium. After the PMA priming, cells were treated with 100 (g/mL SPs for 24 h. The cytotoxicity of the SPs against THP-1 cells was assessed by means of the standard methylene blue assay. In brief, after the SP treatment, cells were fixed with 100 µL of 2.5% glutaraldehyde for 15 min and stained with 100 µL of 0.05% methylene blue for 15 min. Then, the cells were lysed with 200 µL of 0.33 N HCl. The OD<sub>655–415</sub> was measured using a multiwell spectrophotometer (Molecular Devices, Inc., Tokyo, Japan).

For the inhibitory assays, PMA-primed THP-1 cells were pre-incubated with BHA (150 µM) or zVAD-fmk (60 µM) for 30 min and then treated with 100 µg/mL SPs for 24 h in the presence or absence of each inhibitor.

### 3.5. Laser scanning confocal microscopy analysis

THP-1 cells (1.0 × 10<sup>5</sup> cells/well) were seeded on Lab-Tek II Chambered Coverglass (Nunc, Rochester, NY), differentiated to macrophages by incubation with 0.5 µM PMA for 24 h, and treated for 6 h with 100 µg/mL mSP1000s. Then the cells were washed and fixed with 4% paraformaldehyde and mounted with Prolong Gold with 2-(4-amidinophenyl)-1H-indole-6-carboxamide (DAPI, Invitrogen, Carlsbad, CA) for nuclear staining. Fluorescence was observed with a laser scanning confocal microscope (Leica Microsystems GmbH, Wetzlar, Germany).

### 3.6. Statistical analysis

All results are presented as means ± standard deviation (SD). Differences were compared using Student's *t*-test or Scheffé's method after analysis of variance (ANOVA).

Acknowledgements: The authors declare that they have no conflicts of interest. This study was supported in part by grants from the Ministry of Health, Labor, and Welfare in Japan.

## References

Akerman ME, Chan WC, Laakkonen P, Bhatia SN, Ruoslahti E (2002) Nanocrystal targeting *in vivo*. *Proc Natl Acad Sci U S A* 99: 12617–12621.

Albrecht C, Schins RP, Hohl D, Becker A, Shi T, Knaepen AM, Borm PJ (2004) Inflammatory time course after quartz instillation: role of tumor necrosis factor- $\alpha$  and particle surface. *Am J Respir Cell Mol Biol* 31: 292–301.

Bharali DJ, Klejbor I, Stachowiak EK, Dutta P, Roy I, Kaur N, Bergey EJ, Prasad PN, Stachowiak MK (2005) Organically modified silica nanoparticles: a nonviral vector for *in vivo* gene delivery and expression in the brain. *Proc Natl Acad Sci U S A* 102: 11539–11544.

Bottini M, D'Annibale F, Magrini A, Cerignoli F, Arimura Y, Dawson MI, Bergamaschi E, Rosato N, Bergamaschi A, Mustelin T (2007) Quantum

dot-doped silica nanoparticles as probes for targeting of T-lymphocytes. *Int J Nanomedicine* 2: 227–233.

Cho WS, Choi M, Han BS, Cho M, Oh J, Park K, Kim SJ, Kim SH, Jeong J (2007) Inflammatory mediators induced by intratracheal instillation of ultrafine amorphous silica particles. *Toxicol Lett* 175: 24–33.

Cross CE, van der Vliet A, O'Neill CA, Eiserich JP (1994) Reactive oxygen species and the lung. *Lancet* 344: 930–933.

Dostert C, Petrillic V, Van Bruggen R, Steele C, Mossman BT, Tschopp J (2008) Innate immune activation through Nalp3 inflammasome sensing of asbestos and silica. *Science* 320: 674–677.

He X, Nie H, Wang K, Tan W, Wu X, Zhang P (2008) *In vivo* study of biodistribution and urinary excretion of surface-modified silica nanoparticles. *Anal Chem* 80: 9597–9603.

Hirsch LR, Stafford RJ, Bankson JA, Sershen SR, Rivera B, Price RE, Hazle JD, Halas NJ, West JL (2003) Nanoshell-mediated near-infrared thermal therapy of tumors under magnetic resonance guidance. *Proc Natl Acad Sci U S A* 100: 13549–13554.

Hoff T, Spencker T, Emmendoerffer A, Goppelt-Strube M (1992) Effects of glucocorticoids on the TPA-induced monocytic differentiation. *J Leukoc Biol* 52: 173–182.

Huax F (2007) New developments in the understanding of immunology in silicosis. *Curr Opin Allergy Clin Immunol* 7: 168–173.

Kirchner C, Liedl T, Kudera S, Pellegrino T, Munoz Javier A, Gaub HE, Stoltzle S, Fertig N, Parak WJ (2005) Cytotoxicity of colloidal CdSe and CdSe/ZnS nanoparticles. *Nano Lett* 5: 331–338.

Mossman BT, Churg A (1998) Mechanisms in the pathogenesis of asbestosis and silicosis. *Am J Respir Crit Care Med* 157: 1666–1680.

Msiska Z, Pacurari M, Mishra A, Leonard SS, Castranova V, Vallyathan V (2009) DNA double strand breaks by asbestos, silica and titanium dioxide: possible biomarker of carcinogenic potential? *Am J Respir Cell Mol Biol* in print.

Napierska D, Thomassen LC, Rabolli V, Lison D, Gonzalez L, Kirsch-Volders M, Martens JA, Hoet PH (2009) Size-dependent cytotoxicity of monodisperse silica nanoparticles in human endothelial cells. *Small* 5: 846–853.

Roy I, Ohulchanskyy TY, Bharali DJ, Pudarav HE, Mistretta RA, Kaur N, Prasad PN (2005) Optical tracking of organically modified silica nanoparticles as DNA carriers: a nonviral, nanomedicine approach for gene delivery. *Proc Natl Acad Sci U S A* 102: 279–284.

Rutault K, Hazzalin CA, Mahadevan LC (2001) Combinations of ERK and p38 MAPK inhibitors ablate tumor necrosis factor- $\alpha$  (TNF- $\alpha$ ) mRNA induction. Evidence for selective destabilization of TNF- $\alpha$  transcripts. *J Biol Chem* 276: 6666–6674.

Terman A, Gustafsson B, Brunk UT (2006) The lysosomal-mitochondrial axis theory of postmitotic aging and cell death. *Chem Biol Interact* 163: 29–37.

Ting JP, Willingham SB, Bergstralh DT (2008) NLRs at the intersection of cell death and immunity. *Nat Rev Immunol* 8: 372–379.

Verraedt E, Pendela M, Adams E, Hoogmartens J, Martens JA (2009) Controlled release of chlorhexidine from amorphous microporous silica. *J Control Release*.

Waters KM, Masiello LM, Zangar RC, Tarasevich BJ, Karin NJ, Quesenberry RD, Bandyopadhyay S, Teeguarden JG, Pounds JG, Thrall BD (2009) Macrophage responses to silica nanoparticles are highly conserved across particle sizes. *Toxicol Sci* 107: 553–569.

Wiethoff AJ, Reed KL, Webb TR, Warheit DB (2003) Assessing the role of neutrophil apoptosis in the resolution of particle-induced pulmonary inflammation. *Inhal Toxicol* 15: 1231–1246.



二特集

第 80 回日本衛生学会  
連携研究会：繊維・粒子状物質研究会

## ナノマテリアルの安全確保に向けた Nano-Safety Science 研究

吉岡 靖雄<sup>\*1,2,3</sup>, 吉川 友章<sup>\*2,3</sup>, 堤 康央<sup>\*1,2,3</sup>

<sup>\*1</sup>大阪大学臨床医工学融合研究教育センター

<sup>\*2</sup>大阪大学大学院薬学研究科

<sup>\*3</sup>独立行政法人医薬基盤研究所

### Nano-Safety Science for Assuring the Safety of Nanomaterials

Yasuo YOSHIOKA<sup>\*1,2,3</sup>, Tomoaki YOSHIKAWA<sup>\*2,3</sup> and Yasuo TSUTSUMI<sup>\*1,2,3</sup>

<sup>\*1</sup>The Center for Advanced Medical Engineering and Informatics, Osaka University

<sup>\*2</sup>Graduate School of Pharmaceutical Sciences, Osaka University

<sup>\*3</sup>National Institute of Biomedical Innovation

**Abstract** Developments in nanotechnology have fostered the widespread use of a diverse array of nanomaterials such as nanosilicas and carbon nanotubes. Nanomaterials are already being used in electronics, sunscreens, cosmetics, and medicines, because they have unique physicochemical properties, such as conductivity, strength, durability, and chemical reactivity. The advent of nanomaterials has also provided extraordinary opportunities for biomedical applications. However, the increasing use of nanomaterials has raised public concern about their potential risks to human health. In particular, recent reports have indicated that carbon nanotubes induce severe inflammation and mesothelioma-like lesions in mice. In this regard, we have attempted to elucidate the pharmacodynamics and safety of nanomaterials in order to develop novel, safe nanomaterials and to establish scientifically based regulations. In this review, we introduce our data on the safety of nanosilicas, particularly the relationships among their physical properties (predominant grain size, configuration, and surface charge), pharmacodynamics, and safety. Our study will help to improve the quality of human life by establishing standards for the safe use of nanomaterials.

**Key words:** nanomaterial (ナノマテリアル), Nano-Safety Science, nanosilica (ナノシリカ)

#### はじめに

2000年1月に、当時の米国クリントン大統領が「国家ナノテクノロジー戦略」を発表し、大規模国家予算を投資したことが一つの起爆剤となり、ナノマテリアルの開発研究と生産、そして実用化が、国内外の産官学を問わず、多くの領域（医療、情報、環境、エネルギーなど）で急速に進展した。ナノマテリアルとは、少なくとも一

次元の大きさが100 nm以下で製造された超微細材料と定義されている。このナノマテリアルは、従来までのサブミクロンサイズ以上（100 nm以上）の素材とは異なり、サイズ減少に伴う組織浸透性の増大や電子反応性の増大、重量あたりの表面積の増加などにより、抗酸化効果や紫外線遮蔽効果といった有用機能が格段に向上しており、我々の生活の質的向上に革命を起こすものと注目されている。そのため、種々の産業で夢の新素材になるものと期待されており、医薬品・食品・化粧品領域では、ナノシリカやナノ酸化チタン、フラーレン、白金ナノコロイド、ナノシルバーなどが、必須素材として既に上市されている（図1）。

一方で、ナノマテリアルの物性（サイズ、形状など）に起因した革新的機能が逆に、二面性を呈してしまい、

受付 2010年7月31日, 受理 2010年7月31日  
Reprint requests to: Yasuo YOSHIOKA, PhD  
The Center for Advanced Medical Engineering and Informatics,  
Osaka University, 1-6 Yamadaoka, Suita, Osaka 565-0871, Japan  
TEL: +81(6)6879-8177, FAX: +81(6)6879-8177  
E-mail: yasuo@phs.osaka-u.ac.jp

物質名	国内生産量	用途
カーボンナノチューブ	120-140 t	電子材料
カーボンブラック	80万 t	タイヤ、自動車部品等
二酸化チタン	1450 t	化粧品、光触媒等
フラーレン	2 t	化粧品、スポーツ用品等
酸化亜鉛	480 t	化粧品等
非晶質シリカ	9万 t	食品、化粧品、インク、合成ゴム、タイヤ等

図1 主なナノマテリアルの生産量と用途。経済産業省のホームページから一部改変して転載。

サブミクロンサイズ以上の従来型素材では観察されない特徴的な毒性、所謂、ナノトックス (NanoTox) を発現してしまうことが世界的に懸念されている (1-3)。例えば、今後の詳細な検証が必要ではあるものの、カーボンナノチューブや酸化チタンの発がん性・起炎性など、健康被害を示唆する研究報告が相次いでいる (4-6)。そのため、経済協力開発機構 (OECD) と連携しつつ、欧米各国などはナノマテリアルの開発やその利用を規制しようとする動きを加速している。我が国でも、厚生労働省や経済産業省、環境省、内閣府を中心にナノマテリアルの安全性評価研究が今、まさにスタートしたところである。

以上の NanoTox 研究を推進するうえで考慮すべき点は、例えば医薬品・化粧品・食品の場合、老若男女・妊婦・胎児・乳幼児・病人を問わず、あらゆる世代のヒトが一生に渡って曝露され続けることにある。そのため、ナノマテリアルがごく僅かでも体内に吸収され、長期に渡って蓄積され続けると、安全性に大きな問題を招きかねない。しかし、NanoTox 研究の大部分はハザード評価 (毒性の有無) に偏重しているのが現状であり、肝心の“体内吸収性や体内/細胞内動態に関する情報”は、世界的に欠乏している。これは、従来までのサブミクロンサイズ以上の素材で積み重ねられてきた知見に基づき、ナノマテリアルの場合でも曝露されても吸収される筈がないだろうという誤った認識にも大きく影響されている。即ち、このままでは、ナノマテリアルの体内吸収性/体内動態に関する検討がなされぬまま、科学的根拠に乏しい無闇な使用規制が施行されてしまい、ナノマテリアルの有用性を享受した豊かな社会の構築や産業発展が阻害されてしまいかねない。従って、知財技術立国を目指す我が国としては、ナノマテリアルの開発・実用化を闇雲に規制するのではなく、ナノテクノロジーの恩恵を社会が最大限に享受できるよう、ナノ産業の育成や発展を強力に支援しつつ、一方で責任ある先進国、そして健康立国として、ナノマテリアルの安全性を高度に保障し、ヒトの健康環境を確保していかなければならない。すなわち、ナノマテリアルを活用した豊かな社会の構築のためにも、今こそ、どの程度我々はナノマテリアルに曝露され

ているのかといった曝露実態の解明や、生体内に取り込まれたナノマテリアルがどの程度組織に分布するのかといった定量的な体内動態評価、さらに、健康影響に及ぼす閾値追求など詳細な安全性評価が待望されている。

以上の背景を踏まえて我々は、安全なナノマテリアルの創製に向けた基盤情報の収集、使用指針の策定に向け、ナノマテリアルの物性・体内動態・安全性の3者連関を解析することで、健康影響発現に及ぼす閾値の追求・安全なナノマテリアルの設計指針の構築を図ってきた (6-11)。本稿では、我々の取り組みの中から、最も汎用されているナノマテリアルの一つである非晶質ナノシリカの安全性確保研究 (我々は、安全なナノマテリアルの開発研究を推進する視点から NanoTox 研究ではなく、Nano-Safety Science 研究と呼んでいる) について、体内・細胞内動態解析と免疫毒性評価に焦点をあて紹介させて頂き、各方面の先生方からご意見・ご批判を仰ぎたい。

### 非晶質ナノシリカの物性と経皮吸収性との関連評価

非晶質ナノシリカの用途は非常に幅広く、日焼け止めやファンデーションなどの化粧品基材、歯磨き粉や歯の充填剤、食品の固結防止・流動化剤などの食品添加物として利用されている。また、非晶質ナノシリカは食品中に最大2%、化粧品におおよそ20%程度が配合されており、既に我々の生活に必須となっている。さらに近年では、非晶質ナノシリカのサイズダウンや分散性を向上する技術の開発が加速度的に進展しており、直径が2.5 nm程度のもの (所謂、サブナノサイズ) までも開発されつつあり、その使用量・適用範囲は増加の一途を辿っている。従って、非晶質ナノシリカの環境中への流出や廃棄、非晶質ナノシリカ含有製品の使用により、生体が経口、経肺、経皮など、様々な経路で非晶質ナノシリカに、意図的・非意図的な曝露を受ける機会が今後ますます増大していくことは想像に難くない。一方で、その安全性に関する検討は、他のナノマテリアルに比べて圧倒的に遅れているのが現状である。欧州化学物質生態毒性・毒性センターによれば、サブミクロンサイズ以上の非晶質シ

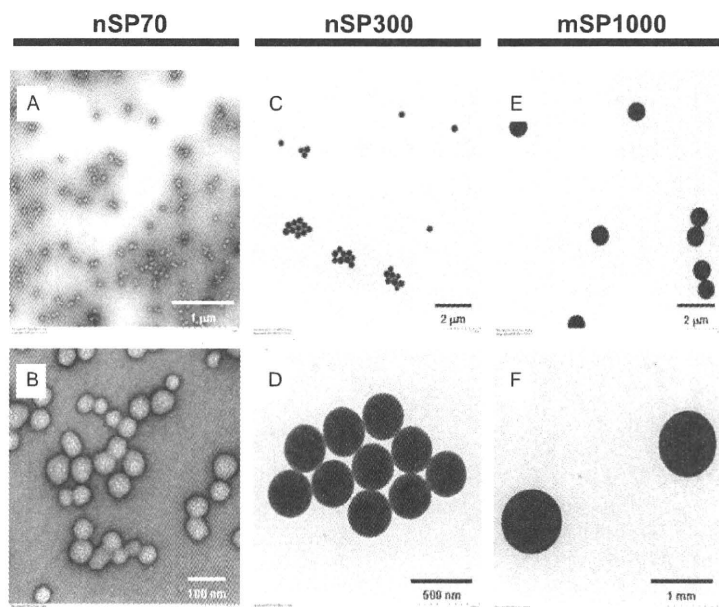


図 2 非晶質シリカの電子顕微鏡写真。(A and B) 直径 70 nm のシリカ (nSP70), (C and D) 直径 300 nm のシリカ (nSP300), (E and F) 直径 1,000 nm のシリカ (mSP1000)。

リカ (一次粒径は 100 nm 以下であっても、凝集体として、サブミクロンサイズ以上になる非晶質ナノシリカを含む) の安全性に問題は無いと報告されている (12)。しかし、この報告は、昨今の分散性に優れた 100 nm 以下の非晶質ナノシリカの安全性を保証するものではない。特に、100 nm 以下の分散性の高い素材に関しては、体内に吸収される可能性が世界的に懸念されており、この点に関する検討が急務となっている。

そこで本研究では、まず、分散性が極めて高い非晶質シリカを用いて、経皮吸収性・体内動態と粒子サイズとの連関を検討した。本研究では、一次粒径が 70 nm の非晶質ナノシリカ (nSP70) 及び、粒子径 300 nm, 1,000 nm の従来型非晶質シリカ (nSP300, mSP1000) を実験に用いた (現在は、30 nm, 50 nm の非晶質ナノシリカやサブナノサイズのものも使用しているが、これらに関しては今後報告させて頂く)。図 2 に非晶質シリカの透過型電子顕微鏡 (TEM) 写真を示す。いずれの粒子も非常に滑らかな形状をした粒子であり、一次/二次粒子径もカタログ値とほぼ同等であった。続いて、nSP70, nSP300, mSP1000 をマウス耳介に塗布した際の経皮吸収性を評価した。各非晶質シリカをマウスに 5 日間あるいは 28 日間連続経皮塗布し、投与局所および所属リンパ節、主要組織への移行を TEM により観察した。その結果、nSP70 が角質層を通過して表皮や真皮層にまで到達し、さらに、所属リンパ節・脾臓や脳内にまで移行することが明らかとなった。特に、リンパ節・脾臓では、リンパ球や貪食細胞であるマクロファージに多く取り込まれることが判明した。なお、従来までのサブミクロンサイズ以上の非晶質シリカである nSP300 や mSP1000 は、表皮層にすら到達しないこと (即ち、高度に安全であること) を確認している。現在は、経口・経鼻・経肺曝露により、nSP70

が投与部位の免疫担当細胞に多く取り込まれるだけでなく、生体内にも吸収されることを明らかとしつつあり、今後より詳細な体内動態を明らかにできるものと考えている。

そこで次に、各非晶質シリカをマウス尾静脈より投与し、非晶質ナノシリカが全身循環した際の動態および生体影響を評価した。まず、種々の粒子径の非晶質シリカの体内動態を蛍光イメージングならびに TEM 解析により評価したところ、nSP300 と mSP1000 は胆嚢に局在する一方で、nSP70 は肝臓全体へ速やかに分布することが明らかとなった (図 3)。また、nSP300 と mSP1000 は肝実質細胞には殆ど移行しないにも関わらず、nSP70 は肝実質細胞へ移行し、最終的に核内にまで到達することが判明した。続いて、各非晶質シリカを 2 mg/head で尾静脈内投与した際の急性毒性を評価した。nSP300 や mSP1000 を静脈内投与したマウスにおいては急性毒性や肝毒性は全く認められなかったのに対して、nSP70 投与マウスは投与後 12 時間以内に全例が死亡した。また、これらのマウスから回収した血液中の肝障害マーカーを測定したところ、100 nm を閾値に粒子サイズの減少により著しい AST や ALT の産生上昇が認められた。これらの結果を重ね合わせると、急性毒性や肝障害性といった生体影響の違いは、非晶質ナノシリカの体内分布特性の差異に起因するものと考えられた。これまで、非晶質ナノシリカが経皮塗布後に体内吸収性や脳内蓄積性を示すといった報告は世界的に見ても皆無である。非晶質ナノシリカが非常に強固な皮膚角質バリアを通過して生体内に移行し、さらに脳をはじめとする各臓器に到達するという事実は非常に興味深く、少なくともこれら的事实は、直径 100 nm 以下の非晶質ナノシリカがサブミクロンサイズの非晶質シリカとは異なる体内/細胞内動態特性を

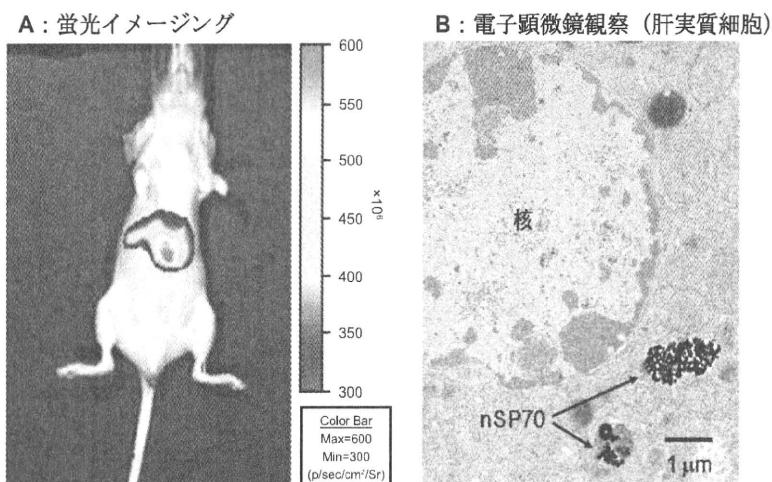


図 3 nSP70 の体内動態解析。DY676 で標識した nSP70 ( $7 \times 10^{10}$  個) を BALB/c マウス (雌, 8 週齢) の尾静脈内より投与した。投与 24 時間後に Xenogen IVIS 200 を用いて nSP70 の局在を蛍光イメージングにより解析した (A)。また、同様に nSP70 を投与したマウスから肝臓を回収し、電子顕微鏡を用いて nSP70 の肝臓内局在を観察した (B)。

発揮する可能性を示している。現在、我々は、安全性評価において最も重要な経皮吸収量 (曝露量) の評価を進めると共に、皮膚透過機構の解析や皮膚局所における安全性評価を推進している。

### 非晶質ナノシリカの細胞内動態と安全性との関連追求

ここまでの検討結果から、直径 100 nm 以下の非晶質ナノシリカがサブミクロンサイズの従来素材とは異なる動態特性を発揮し、ナノマテリアルの動態情報を基盤とした安全性評価が重要であることを明らかにした。そこで次に、非晶質ナノシリカの細胞内動態特性と安全性の関連解析を試みた。まず、ヒト皮膚角化細胞株 (HaCaT 細胞) を用いて、非晶質ナノシリカの細胞内局在を解析した。HaCaT 細胞に各粒子サイズの非晶質シリカを添加し、24 時間後の細胞を TEM で観察した。その結果、nSP300 あるいは mSP1000 作用群では、各シリカが細胞内に侵入した像が認められ、特に mSP1000 作用群においては細菌感染時と同様のリソソーム小胞の過形成を認めた。それに対して、nSP70 は細胞内に侵入するばかりか、核膜を透過して核内に侵入していた。これらの事実は、直径が 100 nm 以下のナノマテリアルが従来までのマイクロメートルサイズのマテリアルとは異なる細胞内動態特性を示すことを裏付けている。即ち、ナノマテリアルの安全性を確保するに当たっては、細胞内取り込み経路や細胞内オルガネラへの到達性、およびその機構などの細胞内動態に関して精査し、それらの情報を基盤とした安全性評価が必須であると考えられる。特に今回使用した非晶質ナノシリカの場合は、核内移行特性を反映した遺伝子や核機能に対する影響の評価が必要であると考えられた。そこで、コメットアッセイにより、非晶質シリカ処理による DNA 損傷の有無を検討したところ、nSP70

作用群においてのみ強力な DNA 損傷効果が認められた。これらの結果は、非晶質ナノシリカが粒子径の減少を反映して細胞傷害や DNA 損傷を誘発し、発がんリスクを増大させ得ることを示している。今後は、nSP70 の核内移行性と DNA 損傷との因果関係を精査すると共に、発がん性試験などを検討する必要があると考えられる。

### 非晶質ナノシリカの起炎性評価および炎症惹起メカニズムの解明

これまでに、生体に取り込まれた粒子状異物排除の根幹を担う免疫担当細胞が、ナノマテリアルを異物として認識した際に、過剰反応や機能不全を起こす可能性が報告されており (6, 13)、ナノマテリアルが未知の免疫攪乱作用を呈する危険性が指摘されている (14)。これらは、ナノマテリアルへの長期・多量曝露が、炎症性疾患や自己免疫疾患、あるいは感染症罹患率の増大など、予期せぬ毒性を引き起こす可能性を示している。我々はこれまでに、サブミクロンサイズの非晶質シリカが、細胞にエンドサイトーシスで取り込まれた後、活性酸素の産生を誘発し、活性酸素がリソソームを破壊することでカテプシン B を細胞質に流出させ、インフラマソームの活性化を誘導することで炎症を惹起することを明らかとしている (15)。しかし、ナノメートルサイズの非晶質ナノシリカの起炎性については、世界的にも明らかとなっていない。さらに上述したように、nSP70 のみ経皮吸収性を有し、その後、リンパ節・脾臓のリンパ球や食食細胞であるマクロファージに多く取り込まれることを明らかとしていることから、nSP70 の免疫機能への影響評価は最優先課題と考えられる。

そこで、粒子径の異なる非晶質シリカの起炎性について、マウスを用いて比較検討した。各粒子径の非晶質シ

リカをマウス腹腔内へと投与し、24時間後における腹腔内の総細胞数を起炎性の指標として評価した。その結果、nSP300, mSP1000 投与群では細胞数の増大はほとんど観察されなかったのに対して、nSP70 投与群においては、有意な細胞浸潤数の増大が認められるなど、非晶質ナノシリカは強い起炎性を有する可能性が示された。さらに、各非晶質シリカ投与2時間後における腹腔内のサイトカイン産生パターンを解析した結果、nSP70 投与群では、炎症性サイトカインやケモカインの産生が認められた。以上の結果より、非晶質シリカは粒子径の減少に従って起炎性が上昇することが明らかとなった。しかし、本結果はあくまでも腹腔内への大量投与による検討であるため、今後、曝露実態を考慮した投与ルートや投与量での検討、更には閾値の解明が必須であると考えられる。

粒子状物質が生体内に取り込まれた場合、まず貪食細胞であるマクロファージに認識されることで免疫応答が誘導される。そこで、代表的なマウスマクロファージ細胞株である RAW264.7 細胞を用いて、非晶質シリカの起炎性を *in vitro* で評価した。RAW264.7 細胞に各非晶質シリカを作用させ、培養上清中に産生される腫瘍壊死因子 (TNF $\alpha$ ) 量を ELISA により評価した。その結果、nSP300, mSP1000 作用群における TNF $\alpha$  の産生量は未処理群とほぼ同程度であったのに対し、nSP70 作用群では有意な TNF $\alpha$  の産生亢進が観察された。本結果より、nSP70 はマクロファージからの TNF $\alpha$  など炎症性サイトカインの産生を誘導することで、炎症を惹起する可能性が示された。

次に、非晶質ナノシリカによる TNF $\alpha$  の産生誘導メカニズムを解析した。細胞が外部からのストレスやサイトカイン刺激を受けると、MAPK ファミリーである p38, c-jun N-terminal kinase (JNK) 及び Extracellular Signal-regulated Kinase 1/2 (ERK1/2) がリン酸化を受けて活性化し、炎症応答や細胞分化、細胞死など、多様な細胞応答に関わるシグナルを伝達することが知られている。そこで、RAW264.7 細胞に各粒子径の非晶質シリカを作用させ、各 MAPK の活性化を評価した。その結果、nSP300, mSP1000 は、いずれの MAPK も活性化しなかったのに対して、nSP70 は全ての MAPK を強く活性化することが明らかとなった。次に、各 MAPK 阻害剤存在下で、nSP70 を RAW264.7 細胞に添加し、TNF $\alpha$  の産生量を ELISA により評価した。その結果、nSP70 単独で作用させた場合、有意な TNF $\alpha$  の産生上昇が認められたのに対し、いずれの MAPK 阻害剤作用条件下においても、nSP70 による TNF $\alpha$  の産生は未処理群と同程度にまで抑制された。本結果は、nSP70 が p38, JNK, ERK1/2 全ての活性化を介して TNF $\alpha$  の産生を誘導することを示すものである (図4)。

#### 起炎性の少ない安全なナノマテリアル開発に向けた取り組み

次に、起炎性の少ない非晶質ナノシリカの開発に向けた基礎情報の集積を目的に、非晶質ナノシリカの表面修

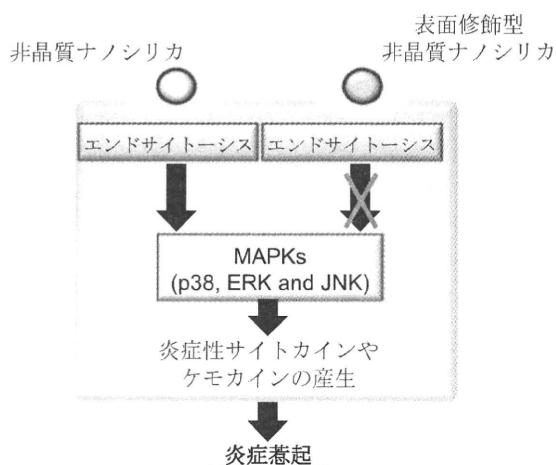


図4 非晶質ナノシリカの起炎性惹起メカニズムの模式図

飾がその起炎性に与える影響を検討した。本検討では、nSP70 の表面をカルボキシル基で修飾した nSP70-C を用いて起炎性を評価した。まず、RAW264.7 細胞を用いて、nSP70 及び nSP70-C の TNF $\alpha$  産生誘導能を比較した。その結果、nSP70 作用群では TNF $\alpha$  の産生量が増加するのに対し、nSP70-C 作用群では全く増加が認められなかった。また、RAW264.7 細胞における MAPK の活性化を評価した結果、nSP70 作用群では、全ての MAPK が活性化されるのに対して、nSP70-C 作用群ではいずれの MAPK の活性化も認められなかった。従って、nSP70 はカルボキシル基修飾によって、MAPK の活性化が強く抑えられた結果、TNF $\alpha$  の産生が大幅に減弱した可能性が示された。さらに、nSP70 及び nSP70-C をマウス腹腔内に投与し、腹腔内の総細胞数を指標に起炎性を評価した。その結果、nSP70 投与群で腹腔内総細胞数が顕著に上昇するのに対し、nSP70-C 投与群は細胞数の上昇はほとんど認められず、未処理群との有意な差は観察されなかった。以上の結果より、nSP70 の有する起炎性は、表面のカルボキシル基修飾によって抑制可能であることが判明した。

#### 終わりに

現在、ナノマテリアルの生体影響に関する詳細な情報を可能な限り早急に収集する必要性が世界的に叫ばれており、OECD では、2006 年から「工業ナノ材料作業部会」を設置し、安全性に対する論議を精力的に進めている。その一方で、ナノマテリアルは人類の QOL 向上に必須の新素材になる可能性を秘めているため、安全性に関するデータが不十分なまま施行された無闇な規制によって、ナノマテリアルの社会受容が阻害され、ひいてはナノマテリアルによって得られるべき恩恵を闇に葬ることは避けねばならない。さらに、種々ナノマテリアル配合製品が既に実用化・販売され、ナノマテリアルの人体曝露を避け得ない現状では、危険性のみを闇雲に指摘する



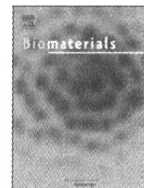
だけでは社会的混乱を招いてしまう。従って、今後、ナノマテリアルが社会から受容され、人類の豊かな暮らしに貢献するためには、適切なリスクマネジメントの実施によって安全性を確保した上で、そのメリットを最大限に享受することが重要である。本研究では、非晶質ナノシリカの皮膚吸収性・体内動態を明らかとした上で、粒子径と急性毒性・起炎性の連関を評価とした。さらに、最も重要なことであるが、適切な物性制御により起炎性を低減可能であることを明らかとした。すなわち、本研究は、単なるナノマテリアルの毒性研究 (NanoTox 研究) を目的としたものでなく、いかにして安全で安心、かつ有用なナノマテリアルを開発・実用化していくのかを視野にいたしたナノマテリアルの安全科学研究 (Nano-Safety Science 研究) を実施したものである。今回は紙面の都合上、割愛させて頂いたが、我々は本項で紹介した検討に加えて、経肺/経口曝露時の体内吸収性・体内動態の解析や、脳神経/免疫/生殖発生学的な Nano-Safety Science 研究を推進しており、既に多くの興味深い知見を得つつある。今後は、ナノマテリアルの曝露実態の解明、定量的な体内動態評価や健康影響に及ぼす閾値追求など詳細な安全性評価を推進するとともに、安全かつ有効なナノマテリアルの開発・実用化支援をより強力に推進することが必要不可欠と考えられる。本稿では紙面の都合上、我々の知見の一例のみ紹介させて頂いたが、これら Nano-Safety Science 研究が、今後のより安全なナノマテリアルの創製・社会還元に関わり、科学的根拠に基づいた情報発信・リスクコミュニケーションにより、リスクリテラシーが高まり、安全で安心な社会の構築などに貢献し得るものと期待している。

## 謝 辞

本研究は、独立行政法人医薬基盤研究所バイオ創薬プロジェクトリーダー 角田慎一先生、同サブリーダー 鎌田春彦先生、同プロジェクト研究員 阿部康弘先生、同プロジェクト研究員 長野一也先生、大阪大学薬学研究科薬剤学分野教授 中川晋作先生、同分野准教授 岡田直貴先生、同分野助教 向 洋平先生、大阪大学大学院薬学研究科毒性学分野講師 伊藤徳夫先生、大阪大学大学院特任助教 鍋師裕美先生、をはじめとする多くの先生方のご指導のもと、遂行されたものであり、この場をお借りして御礼を申し上げます。また当該研究の推進に尽力してくれた学生諸氏に感謝申し上げます。

## 文 献

- (1) Service RF. Nanotoxicology. *Nanotechnology grows up. Science.* 2004;304:1732-1734.
- (2) Kagan VE, Bayir H, Shvedova AA. Nanomedicine and nanotoxicology: two sides of the same coin. *Nanomedicine.* 2005;1:313-316.
- (3) Zhao Y, Xing G, Chai Z. Nanotoxicology: Are carbon nanotubes safe? *Nat Nanotechnol.* 2008;3:191-192.
- (4) Takagi A, Hirose A, Nishimura T, Fukumori N, Ogata A, Ohashi N, Kitajima S, Kanno J. Induction of mesothelioma in p53<sup>+/-</sup> mouse by intraperitoneal application of multi-wall carbon nanotube. *J Toxicol Sci.* 2008;33:105-116.
- (5) Poland CA, Duffin R, Kinloch I, Maynard A, Wallace WA, Seaton A, Stone V, Brown S, Macnee W, Donaldson K. Carbon nanotubes introduced into the abdominal cavity of mice show asbestos-like pathogenicity in a pilot study. *Nat Nanotechnol.* 2008;3:423-428.
- (6) Morishige T, Yoshioka Y, Tanabe A, Yao X, Tsunoda S, Tsutsumi Y, Mukai Y, Okada N, Nakagawa S. Titanium dioxide induces different levels of IL-1beta production dependent on its particle characteristics through caspase-1 activation mediated by reactive oxygen species and cathepsin B. *Biochem Biophys Res Commun.* 2010;392:160-165.
- (7) Yoshikawa T, Nabeshi H, Yoshioka Y. Evaluation of biological influence of nano-materials using toxicokinetic and toxicoproteomic approach. *Yakugaku Zasshi.* 2008;128:1715-1725.
- (8) Yamashita K, Yoshioka Y, Higashisaka K, Morishita Y, Yoshida T, Fujimura M, Kayamuro H, Nabeshi H, Yamashita T, Nagano K, Abe Y, Kamada H, Kawai Y, Mayumi T, Yoshikawa T, Itoh N, Tsunoda S, Tsutsumi Y. Carbon nanotubes elicit DNA damage and inflammatory response relative to their size and shape. *Inflammation.* 2010;33:276-280.
- (9) Nabeshi H, Yoshikawa T, Matsuyama K, Nakazato Y, Arimori A, Isobe M, Tochigi S, Kondoh S, Hirai T, Akase T, Yamashita T, Yamashita K, Yoshida T, Nagano K, Abe Y, Yoshioka Y, Kamada H, Imazawa T, Itoh N, Tsunoda S, Tsutsumi Y. Size-dependent cytotoxic effects of amorphous silica nanoparticles on Langerhans cells. *Pharmazie.* 2010;65:199-201.
- (10) 吉川友章, 吉岡靖雄, 角田慎一, 堤 康央. 化粧品ナノマテリアルの安全性評価の現状と技術的課題～安全なナノマテリアルの開発支援に向けて～. *コスメティックステージ* 2010;4:44-48.
- (11) 吉川友章, 吉岡靖雄, 角田慎一, 堤 康央. 非晶質ナノシリカの経皮吸収性/生体内動態と安全性との連関追求. *ナノ材料のリスク評価と安全性対策.* フロンティア出版, 2010;44-53.
- (12) European Centre for Ecotoxicology and Toxicology of Chemicals, JACC Report. 2006 No 51.
- (13) Mitchell LA, Lauer FT, Burchiel SW, McDonald JD. Mechanisms for how inhaled multiwalled carbon nanotubes suppress systemic immune function in mice. *Nat Nanotechnol.* 2009;4:451-456.
- (14) Dobrovolskaia MA, McNeil SE. Immunological properties of engineered nanomaterials. *Nat Nanotechnol.* 2007;2:469-478.
- (15) Morishige T, Yoshioka Y, Inakura H, Tanabe A, Yao X, Narimatsu S, Monobe Y, Imazawa T, Tsunoda S, Tsutsumi Y, Mukai Y, Okada N, Nakagawa S. The effect of surface modification of amorphous silica particles on NLRP3 inflammasome mediated IL-1beta production, ROS production and endosomal rupture. *Biomaterials.* 2010;31:6833-6842.



## Leading Opinion

Acute phase proteins as biomarkers for predicting the exposure and toxicity of nanomaterials<sup>☆</sup>

Kazuma Higashisaka<sup>a,b,1</sup>, Yasuo Yoshioka<sup>a,b,c,\*,1</sup>, Kohei Yamashita<sup>a,b</sup>, Yuki Morishita<sup>a,b</sup>, Maho Fujimura<sup>a,b</sup>, Hiromi Nabeshi<sup>a</sup>, Kazuya Nagano<sup>b</sup>, Yasuhiro Abe<sup>b</sup>, Haruhiko Kamada<sup>b,c</sup>, Shin-ichi Tsunoda<sup>b,c,d</sup>, Tomoaki Yoshikawa<sup>a,b</sup>, Norio Itoh<sup>a</sup>, Yasuo Tsutsumi<sup>a,b,c,\*\*</sup>

<sup>a</sup> Department of Toxicology and Safety Science, Graduate School of Pharmaceutical Sciences, Osaka University, 1-6 Yamadaoka, Suita, Osaka 565-0871, Japan

<sup>b</sup> Laboratory of Pharmaceutical Proteomics, National Institute of Biomedical Innovation, 7-6-8, Saito-Asagi, Ibaraki, Osaka 567-0085, Japan

<sup>c</sup> The Center for Advanced Medical Engineering and Informatics, Osaka University, 1-6, Yamadaoka, Suita, Osaka 565-0871, Japan

<sup>d</sup> Department of Biomedical Innovation, Graduate School of Pharmaceutical Sciences, Osaka University, 7-6-8, Saito-Asagi, Ibaraki, Osaka 567-0085, Japan

## ARTICLE INFO

## Article history:

Received 8 July 2010

Accepted 31 August 2010

Available online 22 September 2010

## Keywords:

Nanoparticle

Plasma proteins

Silica

Surface modification

## ABSTRACT

Recently, nanomaterials have become an integral part of our daily lives. However, there is increasing concern about the potential risk to human health. Here, we attempted to identify biomarkers for predicting the exposure and toxicity of nanomaterials by using a proteomics based approach. We evaluated the changes of protein expression in plasma after treatment with silica nanoparticles. Our analyses identified haptoglobin, one of the acute phase proteins, as a candidate biomarker. The results of ELISA showed that the level of haptoglobin was significantly elevated in plasma of mice exposed to silica nanoparticles with a diameter of 70 nm (nSP70) compared to normal mice and those exposed to silica particles with a diameter of 1000 nm. Furthermore, the other acute phase proteins, C-reactive protein (CRP) and serum amyloid A (SAA) were also elevated in plasma of nSP70 treated mice. In addition, the level of these acute phase proteins was elevated in the plasma of mice after intranasal treatment with nSP30. Our results suggest that haptoglobin, CRP and SAA are highly sensitive biomarkers for assessing the risk of exposure to silica nanoparticles. We believe this study will contribute to the development of global risk assessment techniques for nanomaterials.

© 2010 Elsevier Ltd. All rights reserved.

## 1. Introduction

With the recent development of nanotechnology, nanomaterials such as silica nanoparticles are beginning to be used on a global scale. In comparison to conventional materials with submicron size, nanomaterials display unique properties such as high levels of

electrical conductivity, tensile strength and chemical reactivity [1]. Nanomaterials have already been used in various fields such as electronic engineering, cosmetics and medicine [2,3]. Because nanotechnology is emerging as a leading industrial sector, humans will be increasingly exposed to a wide range of synthetic nanomaterials with diverse properties.

The increasing use of nanomaterials has raised public concerns about the potential risks to human health [4–6]. For example, it is reported that carbon nanotubes induce mesothelioma-like lesions in mice in a similar way to crocidolite asbestos [7]. Other reports showed that exposure to titanium dioxide particles induce inflammatory responses and lung injury in mice [8,9]. In addition, our group showed that silica nanoparticles with a diameter of 70 nm can penetrate mouse skin and enter the circulatory system (unpublished data). Furthermore our group demonstrated that silica nanoparticles induce severe liver damage after systemic administration [10–12]. However, current knowledge of the potential risk of nanomaterials is considered insufficient. Indeed, concerns about the potential dangers of nanomaterials have led the World Health Organization and the Organization for Economic

<sup>☆</sup> *Editor's Note:* This paper is one of a newly instituted series of scientific articles that provide evidence-based scientific opinions on topical and important issues in biomaterials science. They have some features of an invited editorial but are based on scientific facts, and some features of a review paper, without attempting to be comprehensive. These papers have been commissioned by the Editor-in-Chief and reviewed for factual, scientific content by referees.

\* Corresponding author. The Center for Advanced Medical Engineering and Informatics, Osaka University, 1-6 Yamadaoka, Suita, Osaka 565-0871, Japan. Tel.: +81 6 6879 8230; fax: +81 6 6879 8234.

\*\* Corresponding author. Department of Toxicology and Safety Science, Graduate School of Pharmaceutical Sciences, Osaka University, 1-6, Yamadaoka, Suita, Osaka 565-0871, Japan. Tel.: +81 6 6879 8230; fax: +81 6 6879 8234.

E-mail addresses: [yasuo@phs.osaka-u.ac.jp](mailto:yasuo@phs.osaka-u.ac.jp) (Y. Yoshioka), [ytsutsumi@phs.osaka-u.ac.jp](mailto:ytsutsumi@phs.osaka-u.ac.jp) (Y. Tsutsumi).

<sup>1</sup> These authors contributed equally to the work.

Co-operation and Development to call for an urgent and detailed evaluation of their safety. Therefore, it is extremely important to progress these safety evaluations in order to facilitate the development of nanomaterials that are harmless to humans, because nanomaterials have the potential to improve the quality of human life. In particular, it is hoped that a risk assessment system can be developed to estimate or predict the safety and toxicity of nanomaterials.

Molecular biomarkers, obtained from biological samples such as blood, urine and tissue, constitute an objective indicator for correlating against various physiological conditions or variation of disease state [13,14]. By using biomarkers, we are able to predict not only the present disease and clinical condition but the risk of acquiring disease in the future. Nowadays, biomarkers that act as predictors of cancer have already been developed and are commonly used in clinical practice [14]. Furthermore, such an approach is capable of predicting adverse effects of drugs and medicines [15,16]. By contrast, studies of biomarkers for nanomaterials have barely advanced. These biomarkers would represent the unity of local and systemic physiological responses induced as a result of the exposure. Therefore, biomarkers for nanomaterials will be invaluable for predicting their potential toxicity and establishing strategies for the safe development of nanomaterials production and use.

Here we attempted to develop potential biomarkers of nanomaterials using a proteomics analysis with the aim of developing safe forms of nanomaterials.

## 2. Materials and methods

### 2.1. Materials

Silica particles were purchased from *Micromod Partikeltechnologie* (Rostock/Warnemünde, Germany). The silica particles with diameters of 30, 70, 300 and 1000 nm (nSP30, nSP70, nSP300 and mSP1000, respectively), and nSP70 with surface functional groups such as carboxyl group and amino group (nSP70-C and nSP70-N, respectively) were used in this study. The silica particles were sonicated for 5 min and vortexed for 1 min prior to use.

### 2.2. Animals

Female BALB/c mice were purchased from Nippon SLC, Inc (Shizuoka, Japan) and used at 6–8 weeks of age. All of the animal experimental procedures in this study were performed in accordance with the National Institute of Biomedical Innovation guidelines for the welfare of animals.

### 2.3. Blood sample collection

For administration of silica particles through an intravenous route, BALB/c mice were treated with nSP70, nSP300, mSP1000, nSP70-C, nSP70-N or saline at 0.8 mg/mouse. At various times (6 h, 24 h, 3 day and 7 day) after treatment of these silica particles, blood samples were collected. For administration of silica particles through an intranasal route, BALB/c mice were treated with nSP30, nSP70 or saline intranasally at 0.5 mg/mouse. Blood samples were collected 24 h after the treatment of these silica nanoparticles.

### 2.4. Analysis of biomarkers for nanomaterials using a proteomics approach

BALB/c mice were treated with 0.8 mg/mouse nSP70 or saline intravenously. After 24 h, blood samples were collected and plasma was harvested by centrifuging blood at 12000 rpm for 15 min. Proteo prep (Sigma–Aldrich; Saint Louis, MO) was used to remove albumin and immunoglobulins from the plasma according to the manufacturer's instructions. Plasma samples were then analyzed by sodium dodecyl sulfate-polyacrylamide gel electrophoresis (SDS-PAGE) followed by Coomassie Brilliant Blue staining. Plasma diluted into aliquots corresponding to 10 µg protein were mixed with an equal volume of Laemmli sample buffer (BIO-RAD, Tokyo, Japan) containing 5% 2-mercaptoethanol and boiled for 5 min prior to electrophoresis. Electrophoresis was performed at 15 mA for 10 min (stacking) followed by separation (600 V, 40 mA, 100 W) for approximately 45 min, using Precision Plus Protein Kaleidoscope molecular weight markers (BIO-RAD) as standards.

### 2.5. Identification of candidate proteins as biomarkers

Bands of interest were excised from the gel and then destained with 50% acetonitrile (ACN)/25 mM  $\text{NH}_4\text{HCO}_3$  for 10 min, dehydrated with 100% ACN for 10 min, and then dried using a centrifugal concentrator. Next, 8 µl of 20 µl/ml trypsin solution (Promega, Madison, WI) diluted 5-fold in 50 mM  $\text{NH}_4\text{HCO}_3$  was added to each gel piece and then incubated overnight at 37 °C. We used three solutions to extract the resulting peptide mixtures from the gel pieces. First, 50 µl of 50% (v/v) ACN in 0.1% aqueous trifluoroacetic acid (TFA) was added to the gel pieces, which were then sonicated for 30 min. Next, we collected the solution and added 80% (v/v) ACN in 0.1% TFA. Finally, 100% ACN was added for the last extraction. The peptide solution were dried and resuspended in 10 µl of 0.1% formic acid. The resulting peptide mixture was then analyzed by nano-flow liquid chromatography/tandem mass spectrometry (LC/MS; maXis, Bruker Daltonik GmbH, Bremen, Germany).

### 2.6. Measurement of acute phase proteins

Plasma levels of haptoglobin, C-reactive protein (CRP) and serum amyloid A (SAA) were measured by commercial enzyme-linked immunosorbent assay (ELISA) kits (Life Diagnostics, Inc.; West Chester, PA), according to the manufacturer's instructions.

### 2.7. Statistical analyses

All results are expressed as means  $\pm$  SD. Differences were compared by using the Bonferroni's method after analysis of variance (ANOVA).

## 3. Results

### 3.1. Identification of biomarkers of nanomaterials

We used silica particles as a model nanomaterial because it is one of the most common nanomaterials to have been developed. Silica particles are increasingly being used as additives in cosmetics and foods [17,18]. It is predicted that the global market for silica particles will soon grow to \$2 billion and a ton of silica particles is currently produced worldwide every year. Here, we used silica particles with a diameter of 30, 70, 300 and 1000 nm (nSP30, nSP70, nSP300 and mSP1000, respectively). The mean secondary particle diameters of the silica particles measured by Zetasizer were 33, 79, 326 and 945 nm, respectively (data not shown). The silica particles were confirmed to be well dispersed smooth-surfaced spheres by transmission electron microscopy (data not shown).

Initially, we attempted to identify protein biomarkers in mice by analyzing changes in the level of each plasma protein following treatment with silica nanoparticles using a proteomics approach. BALB/c mice were intravenously treated with nSP70 (0.8 mg/mouse) or saline and then plasma samples were collected 24 h later. Because albumin and immunoglobulins are known to account for the majority of plasma proteins, they were removed from the samples prior to analysis so that variation in the level of other proteins could be more closely monitored. The change of protein levels in plasma after treatment with nSP70 was assessed by SDS-PAGE analysis (Fig. 1). The intensity of a band of molecular mass 37 kDa was more intense in the plasma of nSP70 treated mice than that of saline treated control mice (Fig. 1). The band was excised and analyzed by LC/MS in order to identify the corresponding protein. This analysis identified the induced band after treatment with nSP70 as haptoglobin, one of the acute phase proteins.

### 3.2. The level of haptoglobin after treatment with silica particles

To assess the change of haptoglobin level in plasma after administration of silica particles, BALB/c mice were intravenously treated with nSP70, nSP300 or mSP1000 at 0.8 mg/mouse. We did not use nSP30 in the experiment, because nSP30 induced the toxic side effects after intravenous treatment at this dose. We confirmed that nSP70, nSP300 or mSP1000 at this dose did not induce any

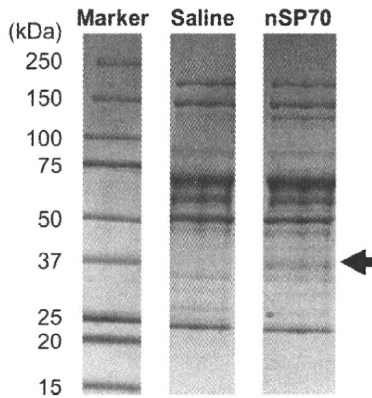


**Fig. 1.** SDS-PAGE analysis of plasma proteins. BALB/c mice were intravenously treated with nSP70 or saline at 0.8 mg/mouse. After 24 h, blood samples were collected. The change of protein levels in plasma after treatment of nSP70 was assessed by SDS-PAGE.

significant elevation of tissue injury and dysfunction markers such as alanine aminotransferase (ALT), aspartate aminotransferase (AST) and blood urea nitrogen (BUN) (data not shown). After 24 h, the level of haptoglobin in the plasma was analyzed by ELISA (Fig. 2A). The levels of haptoglobin in the plasma of nSP70 treated mice were significantly higher than those of saline treated control mice. In contrast, the levels of haptoglobin in the plasma of mSP1000 treated mice were almost the same as those of the saline treated control group. The haptoglobin levels of nSP300 treated mice were slightly higher than those of saline treated control mice. These results indicate that the levels of haptoglobin in the plasma of mice increase as the silica particle size decreases. Thus, haptoglobin appears to be a valuable biomarker for exposure to silica particles of nanometer size.

To assess the potential of haptoglobin as biomarker more precisely, we examined the sensitivity and time dependency of changes in haptoglobin level after treatment with silica particles. BALB/c mice were treated with nSP70, nSP300 or mSP1000 intravenously at 0.8 mg/mouse. After 6 h, 24 h, 3 day and 7 day, we examined the level of haptoglobin in the plasma by ELISA (Fig. 2B). No elevation of haptoglobin in the plasma of mSP1000 treated mice was observed. However, nSP70 and nSP300 treated mice showed a maximum level of haptoglobin 24 h after treatment. Furthermore, at 3 days after treatment, the level of haptoglobin in nSP70 treated mice was significantly higher than saline treated control mice. Next, BALB/c mice were treated with 0.2 and 0.05 mg/mouse nSP70 intravenously. After 24 h, we examined the level of haptoglobin in the plasma by ELISA (Fig. 2C). Mice treated with 0.2 and 0.05 mg/mouse nSP70 did not show any elevated level of haptoglobin. These results indicate that the level of haptoglobin is elevated as the particle size of silica particles decreases and that an increase of haptoglobin is dependent on the concentration of silica particles.

### 3.3. Response of other acute phase proteins

Haptoglobin, CRP and SAA are typical acute phase proteins that are induced during infection and inflammation [19]. To assess the levels of CRP and SAA in plasma after administration of silica particles, BALB/c mice were intravenously treated with nSP70, nSP300 or mSP1000 at 0.8 mg/mouse. After 6 h, 24 h, 3 day and 7 day, we examined the level of CRP (Fig. 3A) and SAA (Fig. 3B) in the plasma of the mice by ELISA. At 6 h and 24 h, both the level of CRP and SAA in the plasma of mice treated with nSP70 was significantly higher than those of the saline treated control mice. Furthermore, the maximum level of CRP in nSP70 treated mice was observed at

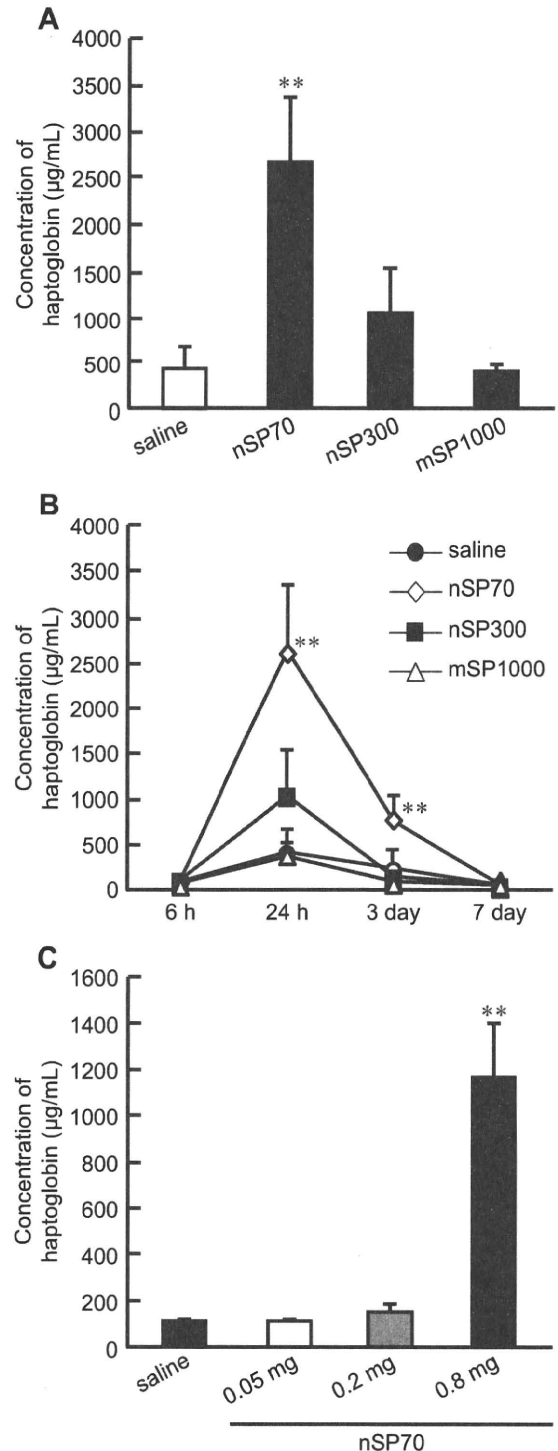


**Fig. 2.** The potential of haptoglobin as biomarker of nanomaterials. (A) The level of haptoglobin after treatment with silica particles. BALB/c mice were intravenously treated with nSP70, nSP300 or mSP1000 at 0.8 mg/mouse. After 24 h, the level of haptoglobin in the plasma of each mouse was examined by ELISA. (B) The time dependency of haptoglobin expression after treatment with silica particles. BALB/c mice were intravenously treated with nSP70, nSP300 or mSP1000 at 0.8 mg/mouse. After 6 h, 24 h, 3 day and 7 day, blood samples were collected. The level of haptoglobin in the plasma of the mice was determined by ELISA. (C) The sensitivity of haptoglobin after treatment of silica particles. BALB/c mice were intravenously treated with nSP70 at 0.8, 0.2 or 0.05 mg/mouse. After 24 h, blood samples were collected. The level of haptoglobin in the plasma of treated mice was determined by ELISA. Data are presented as mean  $\pm$  SD ( $n = 5-6$ ; \*\* $P < 0.01$  versus value for saline treated group by ANOVA).

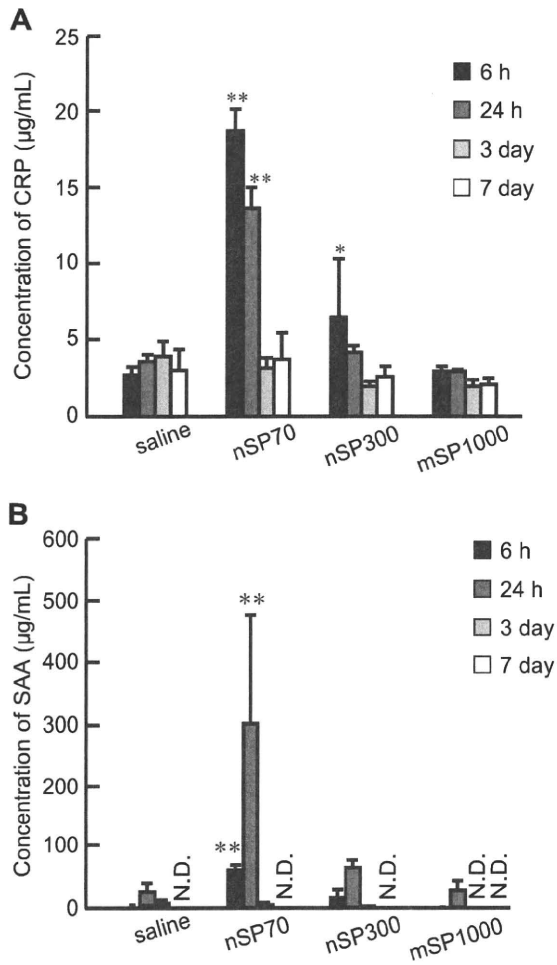


**Fig. 3.** Response of other acute phase proteins. BALB/c mice were intravenously treated with nSP70, nSP300 or mSP1000 at 0.8 mg/mouse. After 6 h, 24 h, 3 day and 7 day, blood samples were collected. The levels of (A) CRP and (B) SAA in the plasma of treated mice were examined by ELISA. Data are presented as mean  $\pm$  SD ( $n = 5-6$ ; \* $P < 0.05$ , \*\* $P < 0.01$  versus value for saline treated group by ANOVA; N.D., not detected).

6 h after treatment, whereas that of haptoglobin and SAA was observed at 24 h. In contrast, the level of CRP and SAA in plasma of mSP1000 treated mice were almost the same as that of the saline treated control mice at all time points. The level of CRP in the plasma of nSP300 treated mice was slightly higher than that of saline treated control mice at 6 h. Our results suggest that both SAA and CRP may be useful biomarkers for predicting the risk from exposure to silica nanoparticles as well as haptoglobin. Indeed, these biomarkers could give even better response and sensitivity when used in combination.

#### 3.4. The level of acute phase proteins through various routes

Exposure to nanomaterials in our daily lives can occur through various different routes. For example, nanomaterials contained in foods and drug medicines are taken up orally, whereas nanomaterials spread in the environment generally enter the body intranasally. Therefore, there is a need to evaluate suitable biomarkers for the exposure of nanomaterials through various routes. To assess the response of acute phase proteins to

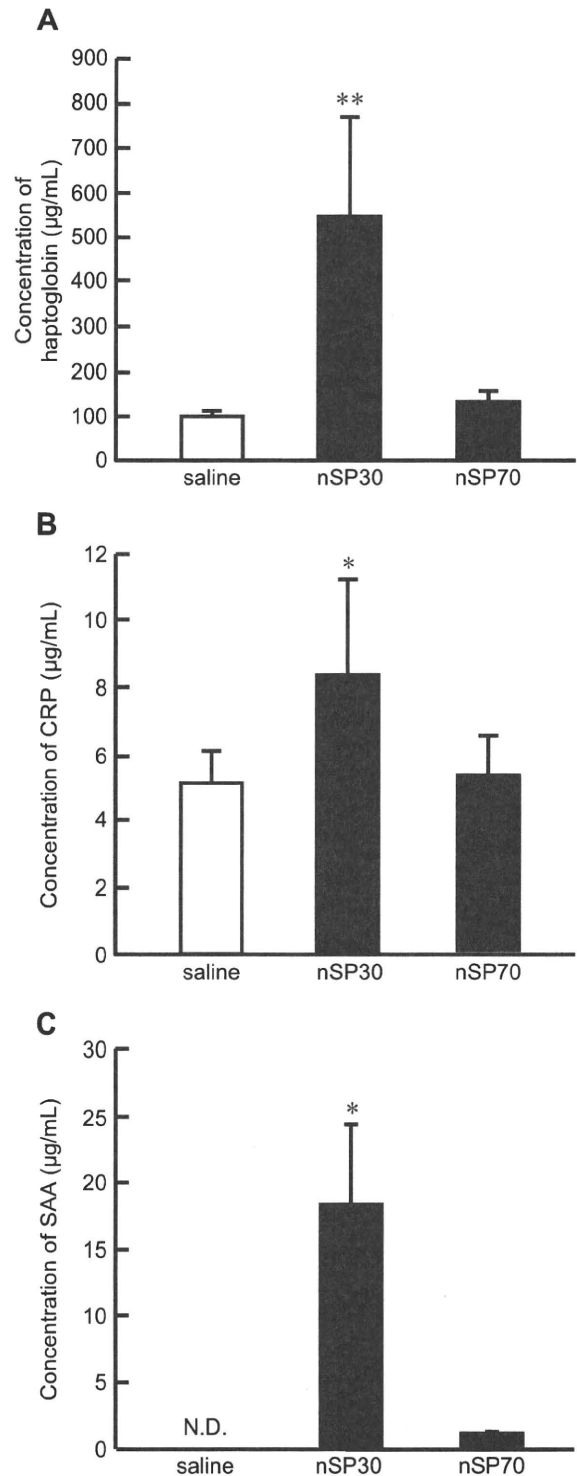


**Fig. 4.** Application of acute phase proteins to assess exposure of nanomaterials through various routes. To assess the administration of silica nanoparticles through an intranasal route, BALB/c mice were treated with nSP30, nSP70 or saline intranasally at 0.5 mg/mouse. Blood samples were collected 24 h after treatment. The level of (A) haptoglobin, (B) CRP and (C) SAA in the plasma were examined by ELISA. Data are presented as mean  $\pm$  SD ( $n = 5-6$ ; \* $P < 0.05$ , \*\* $P < 0.01$  versus value for saline treated group by ANOVA; N.D., not detected).



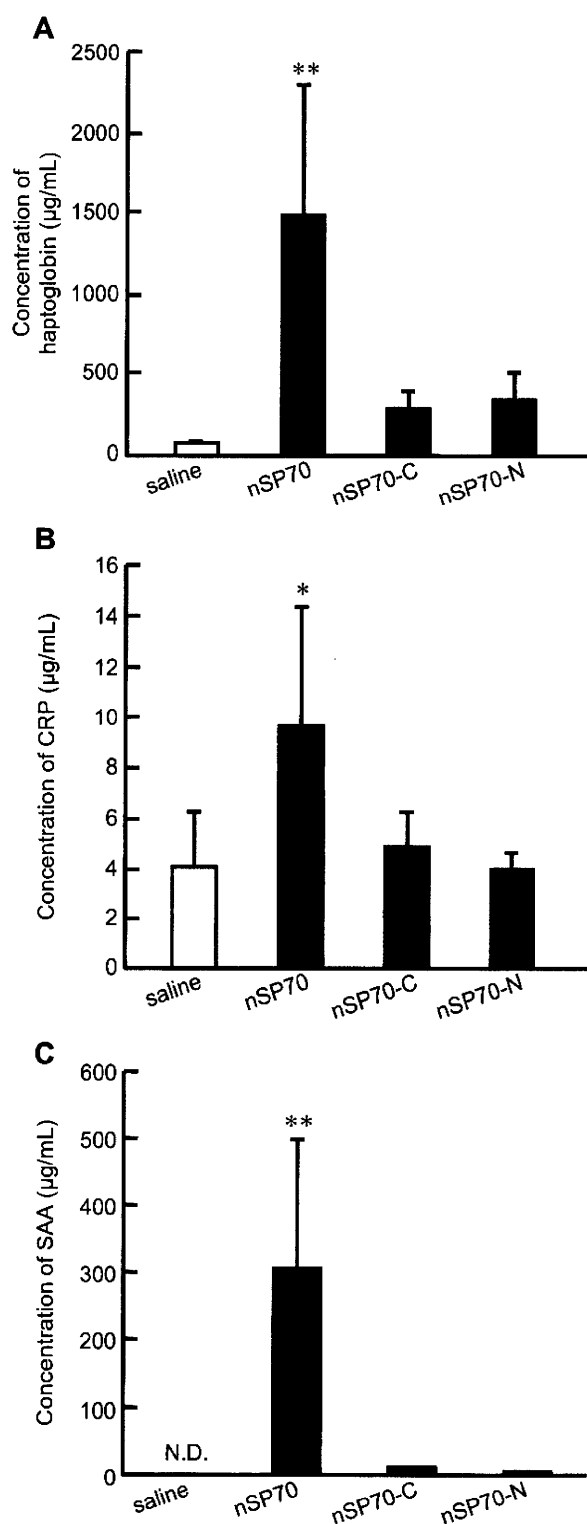


**Fig. 5.** Responses of acute phase proteins by the exposure to surface modified nSP70. BALB/c mice were intravenously treated with nSP70 modified with amino or carboxyl groups at 0.8 mg/mouse. After 24 h, the level of (A) haptoglobin, (B) CRP and (C) SAA in the plasma of treated mice were examined by ELISA. Data are presented as mean  $\pm$  SD ( $n = 5-6$ ; \* $P < 0.05$ , \*\* $P < 0.01$  versus value for saline treated group by ANOVA; N.D., not detected).

silica particles introduced via different routes, we examined the level of haptoglobin, CRP and SAA in plasma after treatment of silica particles intranasally (Fig. 4). In this experiment, we used nSP30 and nSP70. For the administration of silica nanoparticles through an intranasal route, BALB/c mice were treated with nSP30, nSP70 or saline intranasally at 0.5 mg/mouse. After 24 h, we examined the level of haptoglobin (Fig. 4A), CRP (Fig. 4B) and SAA (Fig. 4C) in the plasma of the mice by ELISA. We showed that the level of haptoglobin, CRP and SAA in the plasma of mice treated with nSP30 intranasally was significantly higher than those of the saline treated control mice, although intranasal administration of nSP70 did not cause elevation in the plasma level of each acute phase protein in the treated mice. These results suggest that acute phase proteins could be useful biomarkers for predicting the risk arising from exposure to silica nanoparticles through various routes.

### 3.5. The level of acute phase proteins after treatment with surface modified silica nanoparticles

It has recently become evident that particle characteristics, including particle size and surface properties, are important factors in pathologic alterations and cellular responses [8,20–22]. Previously, our group also showed that surface modification of silica particles with functional groups such as amino or carboxyl group suppressed toxic biological effects of silica particles such as inflammatory responses [23]. To assess whether acute phase proteins could be useful biomarkers to predict risk factors associated with exposure to silica particles, we examined the level of haptoglobin (Fig. 5A), CRP (Fig. 5B) and SAA (Fig. 5C) in the plasma of mice after administration of nSP70 with amino or carboxyl group surface modifications. BALB/c mice were treated with 0.8 mg/mouse of these silica particles intravenously. After 24 h, we examined the level of haptoglobin, CRP and SAA in the plasma of the treated mice by ELISA. Our results showed that the level of these acute phase proteins in the plasma of nSP70 with amino or carboxyl group treated mice were significantly low compared with nSP70 treated mice.

## 4. Discussion

Our goal was to identify the biomarkers of nanomaterials for predicting their potential toxicity and to provide basic information for the creation of safe nanomaterials. To achieve these purposes, we tried to identify biomarkers in blood using a proteomics analysis. At first, we showed that the silica nanoparticles with small particle sizes (diameter  $< 100$  nm) induced a higher level of acute phase proteins such as haptoglobin, CRP and SAA than larger silica particles (diameter  $> 100$  nm) after intravenously treatment (Figs. 2 and 3). Previously, our group has shown that silica nanoparticles with relatively small particle size such as nSP70 induce a greater level of toxicity, including liver injury, compared to those of larger particle size [10,11]. Thus, there is a correlation between toxicity induced by the silica nanoparticles and the level of each potential plasma biomarker. Therefore, these acute phase proteins appear to be good biomarkers for predicting the strength of toxicity induced by silica nanoparticles.

The acute phase response is the nonspecific early response of an organism to infection and inflammation [24]. It comprises a whole array of systemic reactions and induction of a group of serum proteins called the acute phase proteins [25]. Monitoring the progression of infection and cancer by acute phase protein measurements in blood samples is used extensively in human patients. For example, haptoglobin is a biomarker of pancreatic cancer [26]. CRP is used as an index for the development of atrial fibrillation and maintenance [27], although mouse CRP is